Nonlinear averaging in 2D: intraspecific variation in two interacting species and consequences for population dynamics

Koen J. van Benthem [1,†], Rishabh Bagawade [1], Chantal Blüml [1], Peter Nabutanyi [1], Frans M. Thon [1], and Meike J. Wittmann [1]

[1]Department of Theoretical Biology, Bielefeld University, Universitätsstraße 25, 33615 Bielefeld, Germany

[†]Corresponding author: koen.vanbenthem@uni-bielefeld.de

Abstract

Recent empirical and theoretical work shows that intraspecific trait variation (ITV) is prevalent and ecologically important, and should thus be taken into account in ecological models. What is lacking, however, is a comprehensive understanding of the joint effects of ITV in two interacting species (two-dimensional ITV). Here we address this gap for the cases where interspecific individual-by-individual interactions are affected by the trait values of both participants. Using nonlinear averaging in two dimensions, we show for several interaction functions how ITV affects average predation rates or competition coefficients. We develop an intuition for the direction and magnitude of this effect by using a Taylor approximation based on the local curvatures of the interaction function, the trait means, and the trait variances and covariances. We then incorporate the estimated average interaction parameters into simple competition and predator-prey models to derive the expected population-dynamic consequences. We show that two-dimensional ITV can have quantitative effects on abundances, as well as qualitative effects, such as stabilizing or destabilizing coexistence. Our approach can straightforwardly be applied to other interaction functions and dynamical systems and thus provides a valuable tool for understanding the joint effect of trait variation in two interacting species.

1 Introduction

Intraspecific trait variation (ITV) is increasingly being recognized as a factor that can considerably affect population dynamics, community patterns, and global change responses (Bolnick *et al.*, 2011; Violle *et al.*, 2012; Moran *et al.*, 2016; Des Roches *et al.*, 2018). For example, ITV can affect population growth of a single species (Bjørnstad & Hansen, 1994), influence whether or not competing species can coexist (e.g. Hart *et al.*, 2016; Uriarte & Menge, 2018; Hausch *et al.*, 2018; Maynard *et al.*, 2019), and even affect the qualitative outcome of a biological interaction (Moran *et al.*, 2020), i.e. whether it is antagonistic or cooperative.

One important mechanism by which ITV influences population dynamics is nonlinear averaging: when a demographic parameter, e.g. reproductive rate, is a nonlinear function of a certain trait value, the average value of the demographic parameter across individuals is in general not equal to the demographic parameter of an individual with average trait value (Bjørnstad & Hansen, 1994; Ruel & Ayres, 1999, and illustrated in Fig. 1A). In such cases, ITV can lead to directional changes in population-level properties. The direction and magnitude of the effect depend on the curvature of the function relating trait and demographic parameter, according to Jensen's inequality (Jensen, 1905). One can measure this curvature through the second derivative. If the function has a positive second derivative (i.e. is convex), intraspecific trait variation will lead to an increase in the average demographic parameter; and if the function has a negative second derivative (i.e. is concave), ITV will reduce the average demographic parameter.

Here we focus on the effect of ITV on the interaction strength and population dynamics of interacting species. Results on nonlinear averaging have been used to explore the conditions under which ITV promotes or hinders the coexistence of competitors (Gravel *et al.*, 2011; Hart *et al.*, 2016; Uriarte & Menge, 2018) or affects predator-prey dynamics (Okuyama, 2008; Schreiber *et al.*, 2011; Gibert & Brassil, 2014). How ITV plays out in a particular situation can be understood intuitively from the curvature of the interaction function. For example, Hart *et al.* (2016) show for an interspecific competition model that ITV in the sensitivity to competition boosts growth rate because the function linking this trait to fitness has a positive second derivative. In this case, ITV

benefited the superior competitor more and therefore destabilized coexistence. As a second example, Gibert & Brassil (2014) explored the consequences of ITV in a predator's predation efficiency in a Rosenzweig-MacArthur predator-prey model. They used bell-shaped interaction functions with the highest predation efficiency at an intermediate optimum predator trait. Because of the local curvatures of such functions, ITV had a positive effect on average predation rate when the average predator trait was far from the optimum, but a negative effect when the average predator trait was close to the optimum (as in Fig. 1A).

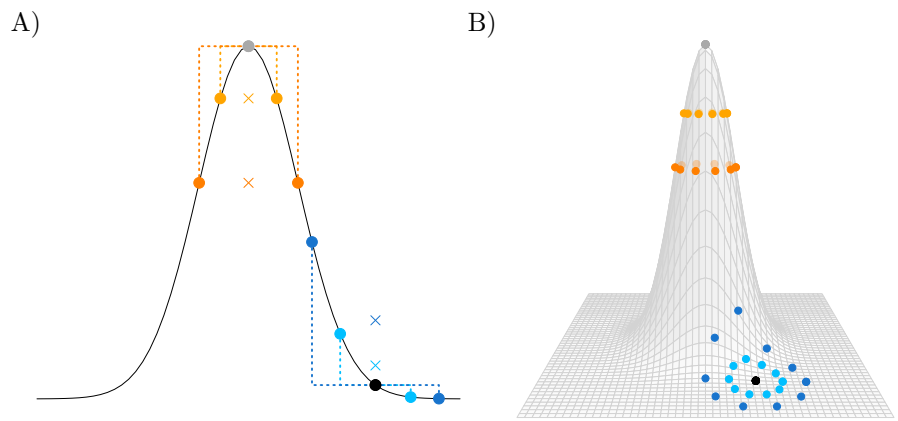

Figure 1 – Illustration of nonlinear averaging in one and two dimensions. A) The values on the x-axis represent trait values, while the height may represent various demographic properties such as per-capita growth rate. The more two points are evenly spread on the $x-$axis around the top (grey point) of a Gaussian function, the more their average height (crosses) decreases (compare the orange and dark orange points and their associated averages). This can be explained by the negative curvature around the maximum. At the base of the Gaussian curve (blue and black points), the function has a positive curvature and therefore the opposite occurs: for two blue points that are equally far from the black, middle point, the point on the left has a much greater increase in height than the decrease for the point on the right. As a consequence, the average height of the blue points is larger than the height of the black point. B) In two dimensions, when trait values vary in two interacting species, similar behaviour occurs: around the maximum of the function (grey dot), the curvatures are negative in all directions and as points are further spread in the $x, y-$plane around the maximum, their average height decreases (orange dots). Towards the base of the function, the curvatures are positive, and the opposite effect occurs and an increase in variation in the traits on the x and y axes (from the black to the dark blue points) leads to an increase in the average height, which may represent for example competition strength or predation rate.

So far, nonlinear averaging theory has provided important insights for scenarios with variation in only one species or scenarios where it is sufficient to consider variation in one species at a time, e.g. because ITV only affects other species indirectly, via population density (e.g. Hart *et al.*, 2016). However, in an interaction between two species, often there is ITV in both species simultaneously and the outcome of an individual-by-individual interaction depends on the exact trait combination of the interacting individuals and this two-dimensional variation can alter the average interaction (as illustrated in Fig. 1B). For example, the performance of plant individuals can depend on their own genotype and traits, but also on the genotype and traits of neighboring interspecific competitors, with complex genotype by genotype (G x G) interactions (Genung *et al.*, 2012). A comprehensive study that describes how ITV in two interacting species affects their population dynamics, through their individual-by-individual interaction, is currently missing.

An additional complexity is that individuals may not always encounter each other randomly. For example, in bank voles and striped field mice, bolder individuals of both species tended to occur more in microhabitats with large maximum vegetation height and a higher percentage of ground cover, suggesting a positive trait covariance among pairs of individuals that are actually interacting (Schirmer *et al.*, 2020).

To our knowledge, so far there is no general theory to quantify the nonlinear averaging effect of ITV in these two-dimensional situations. There are a number of modeling studies that do take into account ITV in two or more species and individual-by-individual variation, e.g. by integrating over interaction kernels (e.g. Barabás & D'Andrea, 2016; Senthilnathan & Gavrilets, 2021) or as part of complex multi-species individual-based models (Banitz, 2019) (see Discussion section). However, these studies have not focused on nonlinear averaging and thus do not make it transparent how the shape of a two-dimensional interaction function and ITV in the interacting species gives rise to the results.

Here, we develop a general framework for nonlinear averaging in two dimensions that can provide an intuitive understanding of the effects of ITV in two interacting species. Our modeling framework accounts for the individual-by-individual nature of ecological interactions and ITV in each of the interacting species, as well as potential trait correlations between co-occurring individuals. We focus

on cases where the overall demographic impact of the interspecific interaction is the sum of many individual-by-individual interactions, but also explore non-additive density-dependent interactions in the supplementary materials. Using our framework, we evaluate how individual variation in each of two interacting species influences their joint ecological dynamics, both in a predator-prey as well as a competition system. We also develop an approximation that can give direct insights regarding the role of ITV and assess the approximation's accuracy under different conditions.

2 General model

We focus on a system of two interacting species A and B where the population-level outcome of the interaction can be thought of as the sum of many individual-by-individual interactions. The outcome of an interaction between a species-A and a species-B individual depends on their respective trait values (a and b respectively). The relation between individual trait values and the outcome of an interaction is given by an interaction function of the form $\gamma(a, b)$ (Fig. 2 top left). For example, $\gamma(a, b)$ could represent the probability that a predator individual of size b successfully captures a prey individual with speed a. Such interaction functions can be estimated from empirical data (Bartomeus *et al.*, 2016).

To determine the ecological consequences of trait variation in the interaction partners, we first determine the average outcome ($\overline{\gamma(a, b)}$) of an interaction across all possible pairs of individuals, weighted by the probability of this pairing given the joint probability distribution $f_{AB}(a, b)$ (Fig. 2). This joint distribution is characterized by the species' mean traits μ_a and μ_b, the trait variances σ_a^2 and σ_y^2, and the trait covariance $\sigma_{a,b}$. Here we think of the covariance as a way to encode spatial co-occurrence patterns, whereas the interaction function encodes the rates and outcomes of interactions given co-occurrence. Note, however, that it is always possible to instead use two independent trait distributions and account for correlations in the interaction function (shown in SI S1).

The average value of $\gamma(a, b)$, $\overline{\gamma(a, b)}$, depends on this distribution function and the shape of γ and is generally not equal to the naive estimate of interaction strength based only on the species

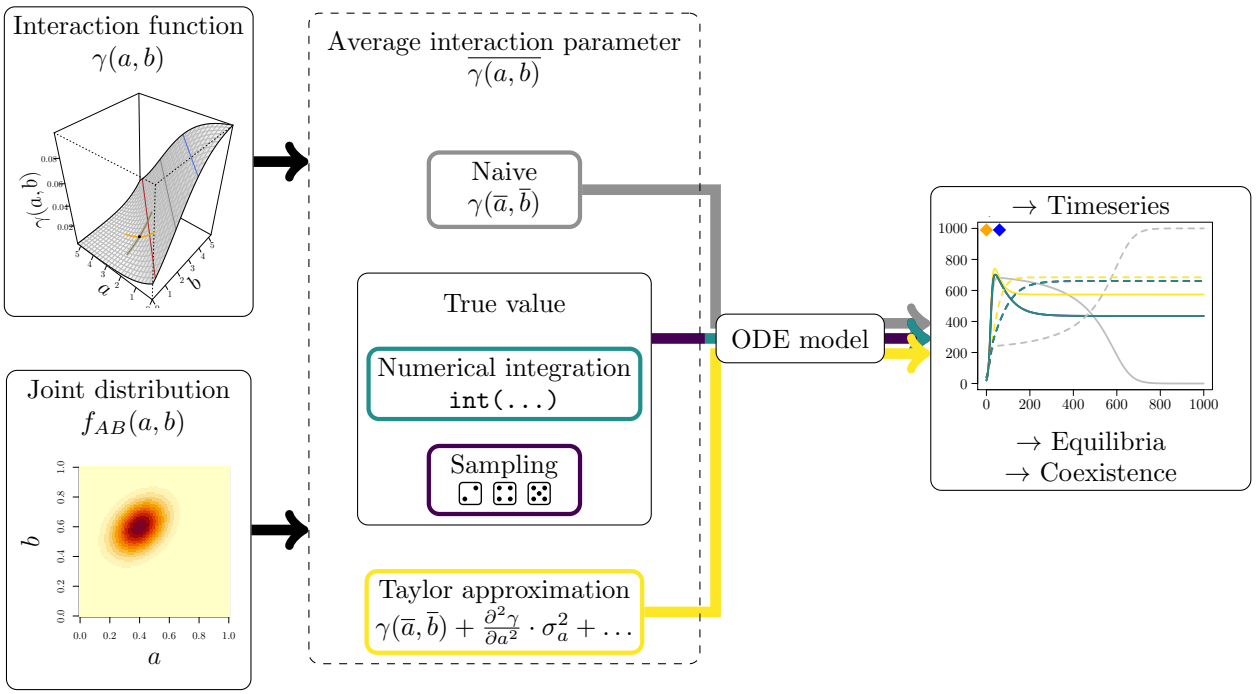

Figure 2 – Overview of the modeling approach. For each analysis, we start with an interaction function that describes the strength (and potentially direction) of the interaction between individuals with trait value a and b and a trait distribution that describes how likely individuals with such trait values are to co-occur. From these two functions, we calculate the average interaction parameter using four different methods (naive, numerical integration, sampling and a Taylor approximation). Finally, we include each estimated value for the average interaction parameter into an ODE model to evaluate the differences in population dynamics that they predict.

mean trait values, $\gamma(\overline{a}, \overline{b})$ (Jensen, 1905). We compare the naive expectation to different approaches for determining $\overline{\gamma(a,b)}$ (Fig. 2, second column). First, we obtain an accurate estimate, either by numerically integrating over the distribution

$$\overline{\gamma(a,b)} = \int\int \gamma(a,b) f_{AB}(a,b) \mathrm{d}a\, \mathrm{d}b \tag{1}$$

using the hcubature routine from the cubature R package (Narasimhan *et al.*, 2019), or by averaging the interaction function over 500,000 trait-value pairs randomly sampled from the joint distribution. This sample size led to acceptably small sampling noise. In the following, we refer to the values from numerical integration and sampling as "true" values, despite the small inaccuracies that they can have due to numerical problems.

Second, we use an approximation based on a second-order Taylor series (SI S2.1):

$$\overline{\gamma(a,b)} \approx \gamma(\overline{a}, \overline{b}) + \frac{1}{2}\gamma_{aa}(\overline{a}, \overline{b})\sigma_a^2 + \frac{1}{2}\gamma_{bb}(\overline{a}, \overline{b})\sigma_b^2 + \gamma_{ab}(\overline{a}, \overline{b})\sigma_{a,b}, \tag{2}$$

where γ_{ij} $(i, j \in \{a, b\})$ are the second order derivatives, or curvatures, of the interaction function with respect to the traits of the species-i and species-j individual respectively. The magnitude of the error of this approximation is of fourth order in deviations from the respective mean traits. Thus, the approximation will fit well as long as most trait values are close to the mean, but might break down for large trait variances. The evaluation of this Taylor approximation is generally less computationally intensive compared to the numerical integration. An added benefit is that the approximation elucidates the role of ITV in the two species and its dependence on the curvature of the interaction function: the larger the magnitude of the curvature, the larger the effect of the associated variation on the average interaction function. A similar Taylor approximation has been used by Chesson & colleagues in their "scale-transition theory" (Chesson *et al.*, 2005; Melbourne & Chesson, 2005; Chesson, 2012) and by Gravel *et al.* (2011) to explore the consequences of spatial and temporal environmental heterogeneity on population dynamics.

After quantifying the effect of ITV on the value of the average interaction parameter $\overline{\gamma}$, we ex-

plore how these differences in interaction estimates affect population dynamics and the population-level outcome of the interaction, e.g. whether the two species are able to coexist or not (Fig. 2 right). First we consider a Lotka-Volterra competition model:

$$\begin{aligned}\frac{\mathrm{d}N_A}{\mathrm{d}t} &= r_A N_A \left(1 - \frac{\alpha_{AA}N_A + \alpha_{AB}N_B}{K_A}\right)\\ \frac{\mathrm{d}N_B}{\mathrm{d}t} &= r_B N_B \left(1 - \frac{\alpha_{BB}N_B + \alpha_{AB}N_A}{K_B}\right),\end{aligned} \tag{3}$$

where N_A and N_B are the population densities of species A and B, r_A and r_B are their intrinsic growth rates and K_A and K_B their carrying capacities. Each of the three competition coefficients can be made dependent on ITV. For example for trait-dependent interspecific competition, this is done by setting $\alpha_{AB} = \overline{\gamma(a,b)}$. Here, we assume that the competition is symmetric, such that the effect of species A on B is the same as the effect of B on A.

Second, we consider a predator-prey model:

$$\begin{aligned}\frac{\mathrm{d}N_A}{\mathrm{d}t} &= r_A N_A (1 - \frac{N_A}{K}) - N_A N_B \phi\\ \frac{\mathrm{d}N_B}{\mathrm{d}t} &= r_B N_B + c N_A N_B \phi,\end{aligned} \tag{4}$$

where N_A and N_B are the prey and predator abundances, $r_A > 0$ and $r_B < 0$ are the prey and predator intrinsic growth rates, K is the environmental carrying capacity and ϕ determines the interaction and is equal to $\overline{\gamma(a,b)}$. Additionally, we explore a Rosenzweig-MacArthur model, in which the interaction function is density-dependent (SI S7.2).

3 Examples

We now illustrate the three described estimation methods on four interaction functions with different patterns of curvature: a general second-order two-dimensional polynomial, a bivariate Gaussian interaction kernel, a logistic interaction function, and a non-differentiable interaction function (Table 1). By comparing the resulting average interaction parameters to the naive value, we determine the

magnitude and direction of the effect of intraspecific trait variation. Furthermore, we also compare the approximation to the "true" estimate to assess the quality of the Taylor approximation. Then, we also explore the resulting consequences for population dynamics. In all examples, we assume that the trait values follow a bivariate normal distribution. Our approach is, however, not limited to a bivariate normal distribution, nor to the used interaction functions.

Table 1 – Overview of the example interaction functions and their second order partial derivatives used in Eq. 2 to approximate $\overline{\gamma(a,b)}$.

Interaction function	$\gamma(a,b)$	$\frac{\partial^2\gamma}{\partial a^2}$	$\frac{\partial^2\gamma}{\partial b^2}$	$\frac{\partial^2\gamma}{\partial a\partial b}$
Polynomial	$p_1a^2 + p_2b^2 + p_3ab + p_4a + p_5b + p_6$	$2p_1$	$2p_2$	p_3
Gaussian	$c_{\max}e^{\frac{-(a-b)^2}{\omega^2}}$	$\frac{4(a-b)^2-2\omega^2}{\omega^4}\gamma(a,b)$	$\frac{\partial^2\gamma}{\partial a^2}$	$-\frac{\partial^2\gamma}{\partial a^2}$
Logistic	$p_{\max}\frac{1}{1+e^{-k(b-a-h)}}$	$k^2(\gamma(a,b) + \frac{2\gamma(a,b)^3}{p_{\max}^2} - 3\frac{\gamma(a,b)^2}{p_{\max}})$	$\frac{\partial^2\gamma}{\partial a^2}$	$-\frac{\partial^2\gamma}{\partial a^2}$
Non-differentiable*	$p_{\max} - c_1b - (d_{\max} - c_2b)a^2$	$-2(d_{\max} - c_2b)$	0	$2c_2a$
	$p_{\max} - c_1b$	0	0	0

* The non-differentiable interaction function is a special case, in which $\gamma(a,b)$, a, b, and $d_{\max} - c_2b$ are forced to be non-negative: whenever one of these terms is negative, that term is set to zero. The effect of this procedure depends on the order of checking the terms and setting them to zero, in our case we first test a, b and $d_{\max} - c_2b$, and $\gamma(a,b)$ itself is checked last. In the table, two cases are shown: on the fourth row of the table, the case is shown where none of the checked values was below zero, and on the fifth row the case where $d_{\max} - c_2b$ was initially below zero.

3.1 Effect of trait variation on the average interaction parameter

The first interaction function we explore is a *two-dimensional polynomial of second order*:

$$\gamma(a,b) = p_1a^2 + p_2b^2 + p_3ab + p_4a + p_5b + p_6. \tag{5}$$

Depending on the parameter values (p_i), this interaction function is shaped as a plane, paraboloid, or a saddle. Since the sign of the interaction changes with the trait values, it can for example be used to describe predator-prey reversal. However, the interaction function is not bounded, and when using it, one should verify that it takes reasonable values over the range of trait values consid-

ered. Alternatively, one might want to introduce bounds as we have done for the non-differentiable interaction function below.

Using the partial derivatives from Table 1, we obtain an approximation for the average interaction parameter:

$$\overline{\gamma(a,b)} = \gamma(\overline{a},\overline{b}) + p_1\sigma_a^2 + p_2\sigma_b^2 + p_3\sigma_{a,b}. \tag{6}$$

Since the third and higher order derivatives are zero for this interaction function, the approximation is exact (see also SI S2.2). The magnitude and the direction of the effect that variation in a and b and their mutual covariance have on $\overline{\gamma(a,b)}$ depend directly on p_1, p_2, and p_3, respectively. If, for example, all three coefficients are zero, the interaction function is linear in a and b, and intraspecific variation has no effect on $\overline{\gamma(a,b)}$. Accordingly, the naive expectation, the true values and the approximation largely coincide (Fig. 3a), with two exceptions. First, small deviations arise in the sampling method due to its inherent stochasticity (e.g. Fig. $3a_{2-3}$). This effect actually occurs in all panels of Fig. 3, but in the other panels these effects are much smaller than the systematic effects of variation on $\overline{\gamma(a,b)}$, rendering them invisible. Second, the numerical integration may fail when variation is low and correlation is strong (Fig. $3a_4$ bottom left). More generally, the efficiency and accuracy of numerical integration methods depend on the shape of the integrand.

If, on the other hand, p_1 and p_2 are negative, while p_3 is moderately positive, variance in a and b both always have negative effects on the average interaction function $\overline{\gamma(a,b)}$, although the effect is weakened when the traits co-vary positively (Fig. 3b). For the specific example in Fig. 3b, $\overline{\gamma(a,b)}$ increases with increasing covariance (Fig. $3b_4$, with bars becoming less negative with increasing $\rho_{a,b}$). However, in SI S3 we show that for the particular interaction function in Fig. $3b_4$, increasing covariance can never change the sign of the effect of ITV from negative to positive, though this is possible with other parameter values. The observed negative effects are expected because the function has negative curvature everywhere and is thus concave, i.e. the line connecting any two points on the graph lies below the graph. The function itself has a single peak at (0,0). Biologically, an interaction function of this general shape could for example represent a mutualism that only works for a specific trait combination and, away from this point, mutualism is weakened or even turns into competition.

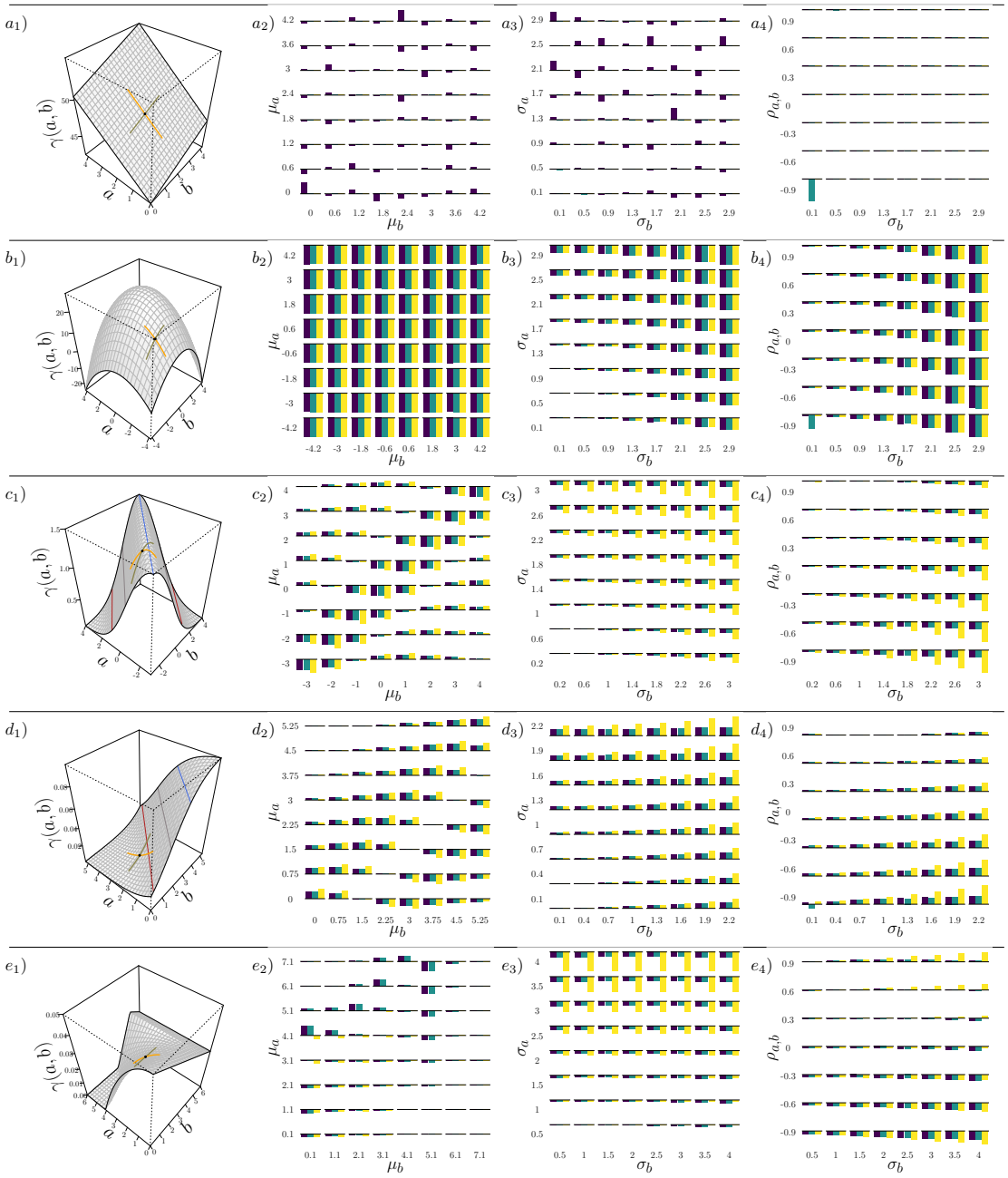

Maximum change

	2	3	4
a	0%	0%	0%
b	5%	40%	28%
c	17%	53%	50%
d	7%	17%	17%
e	18%	14%	17%

Figure 3 – Effect of ITV on the average interaction parameter for various interaction functions, as quantified by the difference between the naive estimate and three estimates that take into account ITV. Left column: illustrations of the interaction functions γ, with orange and brown lines representing a distance $\sigma_a = 1$ and $\sigma_b = 1$ in either direction from the reference point in black. For the Gaussian and logistic interaction functions, lines of zero (grey), maximal (red) and minimal curvature (blue) are shown. The other columns show the difference between the various estimates of $\overline{\gamma(a,b)}$ and the naive estimate $\gamma(\overline{a},\overline{b})$ for differently parameterized trait distributions. The scale of the bars is different across panels. The table at the bottom left indicates for each panel the maximal deviation of the sampling estimate from the naive prediction as a fraction of the range that the γ values take in the illustration in the first column. A value of 100% would thus indicate that including trait variation can cause the same maximal change in average interaction value as ignoring trait variation whilst moving the trait means around the shown trait space. Unless stated differently on the axes, $\overline{a}$ and $\overline{b}$ are at their respective reference values (represented by the cross), $\sigma_a = \sigma_b = 1$ and $\sigma_{a,b} = 0$. (a) Polynomial with $p_1 = p_2 = p_3 = 0$, $p_4 = 2$, $p_5 = 1$ and $p_6 = 42$, at $\mu_a = 2$, $\mu_b = 2$. (b) Polynomial with $p_1 = -1$, $p_2 = -1.5$, $p_3 = 0.5$, $p_4 = p_5 = 0$ and $p_6 = 28$, at $\mu_a = -2.67$, $\mu_b = -2$. (c) Gaussian with $c_{\max} = 1.5$ and $\omega = 3$ at $\mu_a = -1$, $\mu_b = -1.5$. (d) Logistic with $p_{\max} = 0.1$, $k = 1$, $h = 1.5$ at $\mu_a = 2.5$, $\mu_b = 2$. (e) Non-differentiable with $p_{\max} = 0.05$, $d_{\max} = 0.003$, $c_1 = 0.004$ and $c_2 = 0.0006$, at $\mu_a = 2.5$, $\mu_b = 2.5$.

Interestingly, although the value of the interaction changes with the mean trait values, the difference between the naive value and the other estimates only depends on σ_a, σ_b and $\sigma_{a,b}$ (Fig. 3b_2). This is reflected by the constant second derivatives of γ (Table 1). As expected, the results from numerical integration over the interaction function agree with the Taylor approximation (Fig. 3a–b).

For the remainder of this section, we will focus on interaction functions that are bounded between zero and some positive value such that a change in trait value can change the magnitude of the interaction function, but not its sign.

First, we consider a *Gaussian interaction function* that is commonly used in ecological and evolutionary models, for example to model the attack rate of predators or parasites, the strength of competition, or the strength of mutualisms that depend on matching traits (e.g. Gibert & Brassil, 2014; Barabás & D'Andrea, 2016; Hart *et al.*, 2016; Senthilnathan & Gavrilets, 2021). The strength of the interaction decreases with increasing trait difference between the interacting individuals:

$$\gamma(a,b) = c_{\max} e^{\left(\frac{-(a-b)^2}{\omega^2}\right)}, \tag{7}$$

where $c_{\max}$ is the maximum possible interaction coefficient and ω the width of the Gaussian curve

(Fig. $3c_1$).

When the difference in trait values is small compared to the interaction width ω, the curvature is negative (Fig. $3c_1$, the blue line indicates minimum curvature). Thus, when the species' trait means are close together, the $\overline{\gamma(a,b)}$ values that take into account intraspecific variation are lower than the naive estimate (along the diagonal of Fig. $3c_2$) and this effect becomes stronger with increasing trait variation in either species (Fig. $3c_3$). Intuitively this occurs because variation introduces individuals that are more different from the bulk of individuals in both A and B, thereby reducing the average similarity between the species. However, when trait values lie further apart, curvatures are positive (with red lines in Fig. $3c_1$ indicating maximum curvature), and the effect of ITV is reversed (upper left and lower right in Fig. $3c_2$). Here, ITV increases similarity and thereby average interaction strength. With increasing ω, the interaction becomes less trait-dependent and values of $\overline{\gamma(a,b)}$ approach $\gamma(\overline{a},\overline{b})$, as is evident from the vanishing curvatures as ω goes to infinity (see Table 1). At this limit, interaction strength is maximal, since $\lim_{\omega\to\infty}\gamma(a,b) = c_{\max}$.

The Gaussian interaction function can be written purely in terms of the difference between trait values a and b. As shown in SI S4, for such interaction functions the approximation becomes:

$$\overline{\gamma(a,b)} \approx \gamma(\overline{a},\overline{b}) + \left.\frac{\partial^2\gamma}{\partial a^2}\right|_{(\overline{a},\overline{b})}\left(\frac{1}{2}\sigma_a^2 + \frac{1}{2}\sigma_b^2 - \sigma_{a,b}\right) \tag{8}$$

Since, $\frac{1}{2}\sigma_a^2 + \frac{1}{2}\sigma_b^2 - \sigma_{a,b}$ is always positive (SI S4), the sign of the effect of ITV depends solely on $\left.\frac{\partial^2\gamma}{\partial a^2}\right|_{(\overline{a},\overline{b})}$. Furthermore, the variances in a and b contribute equally to a divergence of $\overline{\gamma(a,b)}$ from the naive mean $\gamma(\overline{a},\overline{b})$. This is evidenced by the symmetry across the diagonal of Fig. $3c_3$. The divergence is enhanced if the traits are highly and negatively correlated (Fig. $3c_4$), while the effect of ITV on the interaction function cancels out if the traits are perfectly correlated (correlation coefficient $\rho_{a,b} = 1$) and the trait variances are the same.

Another interaction function that can be written in terms of the difference in trait values is the *logistic function* (see Table 1). The function can, for example, represent the probability of a predator eating a prey when predation success increases with increasing predator size relative to

prey size. This interaction function can be represented as

$$\gamma(a,b) = \frac{p_{\max}}{1+e^{-k(b-a-h)}}, \tag{9}$$

where $p_{\max}$ is the maximum predation rate, h is the difference in traits at which the predation rate is half the maximum and k determines the steepness of the curve. As noted above, because the function only depends on the difference between a and b, σ_x and σ_y have identical effects on $\overline{\gamma(a,b)}$, as evidenced by the symmetry around the diagonal in Fig. $3d_3$.

The interaction function has a region where the curvature is positive with respect to both trait values and a region where the curvature is negative with respect to both trait values, separated by the inflection line $b-a=h$ (grey line in Fig. $3d_1$), at which the curvatures vanish. Therefore, the naive mean will under- or overestimate the mean of $\gamma(a,b)$ depending on the mean trait values (Fig. $3d_2$). When the average predator is smaller than than average prey size plus h, intraspecific trait variation in either species increases the predator's hunting success, and the effect on the approximation is the strongest when $\overline{a} = \overline{b} - h + \frac{\ln(2+\sqrt{3})}{k}$ (red line in Fig. $3d_1$, SI S5.2). Overall hunting efficiency is low in this case, but trait variation yields occasional encounters between predators that are larger than average with relatively small prey items, increasing overall hunting success. This effect can be enhanced with a negative correlation (Fig. $3d_4$): in this case small predators are matched to large prey and basically obtain no food, but this is more than compensated by large predators being matched to small prey that they can feed on efficiently. The effect of ITV on the average interaction parameter is reversed when the average predator is more than h larger than the average prey, with a maximum effect size in the approximation when $\overline{a} = \overline{b} - h - \frac{\ln(2+\sqrt{3})}{k}$ (blue line in Fig. $3d_1$, SI S5.2). The effect of trait variation vanishes when either the average difference becomes very large, or when the trait means are on the inflection line, in which cases trait variation has no effect on the average interaction function and its value should be equal to the naive estimate.

Finally, to illustrate that our approach can also be applied to complex, unconventional 2D interaction functions, we consider a *non-differentiable* interaction function, which is inspired by a system where predators feed on prey that may be toxic. For example, the ability of snakes to feed

on cane toads depends on the body size of the snake, which determines its susceptibility to toxin, and the body size of the toad, which predicts its toxicity (Phillips *et al.*, 2003; Phillips & Shine, 2004). We assume selection has acted on the gape width, such that snakes cannot ingest a prey item that would be lethal to them. As a consequence, the rate of successful attack γ depends on the toxicity of the prey (a) and the resistance to toxicity of the predator (b):

$$\gamma(a,b) = \left((p_{\max} - c_1 b^+) - (d_{\max} - c_2 b^+)^+ a^{+2}\right)^+, \tag{10}$$

with $x^+ \equiv \max(x, 0)$. The actual predation rate is $p_{\max}$ at most, and decreases with the squared toxicity of the prey (a^2) multiplied with a sensitivity factor. This sensitivity factor has a maximum of $d_{\max}$, but decreases with predator toxin resistance, by an amount $c_2 b$. However, the maintenance of the resistance leads to a lower overall predation efficiency (by an amount $c_1 b$). As a consequence, defense against toxicity only pays off when toxic prey is encountered. Furthermore, any negative values of a, b, $\gamma(a,b)$ and $d_{\max} - c_2 b$ are treated as zero, to ensure biologically realistic behavior. This leads to an interaction function that is non-differentiable, for example when $d_{\max} = c_2 b$ or $b = 0$. Around these lines, the derivatives and curvatures are discontinuous.

In our example, the "true" estimates show strong effects of ITV when trait means are close to the discontinuities (Fig. 3e_2). However, in such cases the approximation performs poorly, because it cannot capture dynamics across a discontinuity. Further away from the discontinuities, the approximation again performs satisfactorily. In particular, when predators are very large, to the extent that they are completely immune to the toxin, the interaction function is linear due to the cost of resistance. As a consequence, trait variation does not affect the average interaction here, and hence the naive value and the other estimates are identical (Fig. 3e_2, $\mu_b = 7.1$). Because the system contains only linear terms in b, variation in b has direct effects only through the discontinuities (which cannot be captured by the approximation, Fig. 3e_3). However, variation in b can have indirect effects, also on the approximation, through covariance with the prey trait, which can sometimes be strong enough to overpower the direct effect of variation in a (Fig. 3e_4). Non-differentiable interaction functions such as this one may occur in nature when there are hard bounds on the interaction

function. Even if such limits are approached more smoothly, large changes in curvature may occur within a very small trait value range and the approximation of the effect of ITV in such a region would be inaccurate, as for a non-differentiable function.

3.2 Effect on population dynamics

We have seen that ITV can either increase or decrease the average interaction parameter between two species, $\overline{\gamma(a,b)}$. To evaluate how trait variation affects population dynamics and species coexistence, we incorporate the values of $\overline{\gamma(a,b)}$ into ODE models. For this part of the analysis, we illustrate the results using the logistic interaction function for the predator-prey model and the Gaussian interaction function for the competition model. Note, however, that the results depend directly only on changes in $\overline{\gamma(a,b)}$ and therefore can easily be transferred to other interaction functions.

3.2.1 Lotka-Volterra competition model

In our analysis of the Lotka-Volterra competition model, we first assume that ITV affects only the interspecific competition strength, while the intraspecific competition strength is fixed. That is, we substitute $\overline{\gamma(a,b)}$ for α_{AB} in Eq. 3, and set $\alpha_{AA} = \alpha_{BB} = 1$. According to classical analytical results (see e.g. Begon *et al.*, 2006, and SI S6.1–S6.2), the two competing species in this model can coexist if

$$\alpha_{AB} < \min\left(\frac{K_A}{K_B}, \frac{K_B}{K_A}\right). \tag{11}$$

Thus we obtain a single threshold parameter that determines coexistence. The maximal value of this threshold is 1, and occurs when the species' carrying capacities are equal. A necessary, but not sufficient condition for coexistence is thus $\alpha_{AB} < 1$, which occurs when intraspecific competition is stronger than interspecifc competition, a classical result.

When interspecific competition (α_{AB}) is described by a Gaussian interaction function, trait variation can either increase or decrease average competition, depending on the trait means, as shown in Fig. 4A. Close to the blue diamond, the absolute difference in species' mean trait values

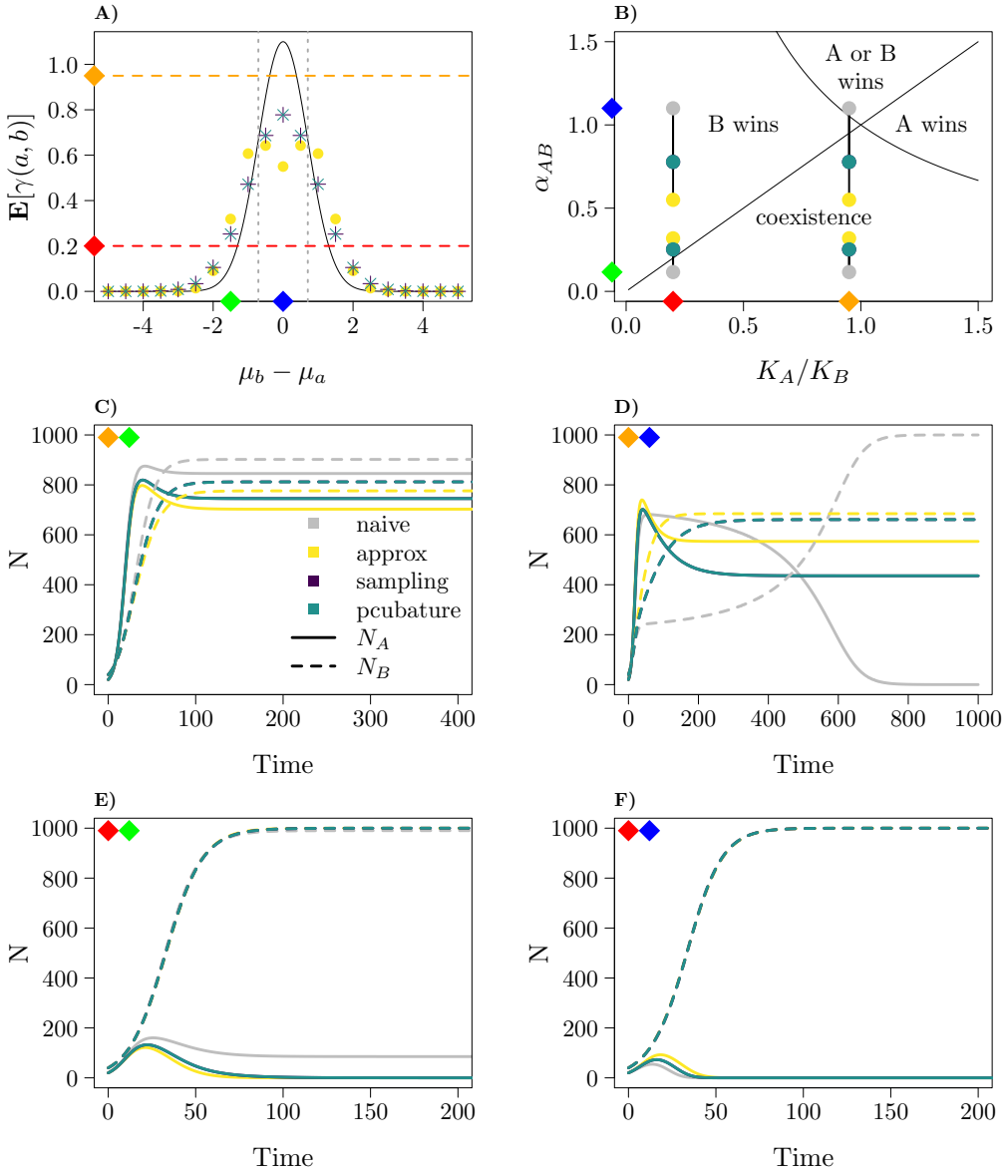
A)
B)
C)
D)
E)
F)
$\mathbf{E}[\gamma(a,b)]$
$\mu_b - \mu_a$
α_{AB}
K_A/K_B
A or B wins
B wins
A wins
coexistence
N
Time
naive
approx
sampling
pcubature
N_A
N_B

Figure 4 – Effect of ITV on the dynamics of the Lotka-Volterra competition model. A) Effect of ITV on the average value of a Gaussian interaction function ($c_{\max} = 1.1, \omega = 1$). Crosses and points indicate the average interaction function when $\sigma_A = \sigma_B = 0.5$ and $\sigma_{a,b} = 0$ (turquoise, purple, and yellow for the pcubature (numerical integration), sampling, and approximation method respectively). The orange and red lines indicate two possible coexistence thresholds (Eq. 11) for $K_A = 950$ and $K_A = 200$, respectively. The green and blue diamonds indicate two trait difference values that are explored in detail in the following panels. The dotted vertical lines indicate $\pm\omega/\sqrt{2}$, the points where the second derivative vanishes. B) Parameter space plot. The different regions are demarcated by the lines $\alpha = K_A/K_B$ and $\alpha = 1/(K_A/K_B)$ C–F) Example time series. The diamonds in the upper left corner indicate the underlying trait difference and threshold value (K_A/K_B). Other parameters: $r_A = 0.2, r_B = 0.1, K_B = 1000$.

is smaller than $\omega/\sqrt{2}$. Here the curvatures are negative and the naive estimate (grey line) is always higher than the estimates that take ITV into account (yellow dots for the approximation and purple and turquoise crosses for the "true" estimates). Whether the effect is strong enough to promote coexistence further depends on the value of the coexistence threshold (orange and red lines and diamonds in Fig. 4). When the threshold is slightly below the naive estimate, effects of trait variation can push the average competition below the threshold and foster coexistence (orange threshold, Fig. 4B,D). On the other hand, if the difference in species' trait means is larger than $\omega/\sqrt{2}$ (green diamond), ITV increases the average competition between the species. When the coexistence threshold (red line in Fig. 4A) is just above the naive value, it can hence destabilize coexistence (e.g. Fig. 4B,E). Not only qualitative changes (Fig. 4B), but also quantitative changes in equilibrium densities emerge through ITV (e.g. Fig. 4C). ITV-driven increases of average competition strength always decrease the equilibrium abundance of the species with the smaller carrying capacity, but can either increase or decrease the equilibrium abundance of the species with the larger carrying capacity depending on the parameter values (SI S6.2).

Second, we consider the case where both interspecific competition parameter (α_{AB}) and intraspecific competition parameters (α_{AA} and α_{BB}, see Eq. 3) are affected by ITV and calculated using the average interaction parameter estimation methods (see SI S6.3). The condition for coexistence is now $\frac{\alpha_{AB}}{\alpha_{BB}} < \frac{K_A}{K_B}$ and $\frac{\alpha_{AB}}{\alpha_{AA}} < \frac{K_B}{K_A}$ (see SI S6.1) which reduces to Eq. 11 when the intraspecific competition strengths (α_{AA} and α_{BB}) are fixed and set to 1. When $K_A = K_B$, the condition for coexistence corresponds to $\alpha_{AB} < min(\alpha_{AA}, \alpha_{BB})$ which implies again that intraspecific competition must be stronger than interspecific competition.

When adding the effect of ITV on intraspecific competition, the coexistence regions generally shrink (compare first and second row, Fig. 5). While with fixed intraspecific competition, ITV could promote coexistence when the trait means were close together (see Fig. 4B,D and upper right corner in Fig. 5), this generally does not occur with trait-dependent intraspecific competition. These observations are consistent across a range of ω and $c_{\max}$ (see Fig. S6.2) and can be explained by the fact that ITV can only decrease intraspecific competition, while coexistence occurs when intraspecific competition is larger than interspecific competition. Neglecting effects of ITV on intraspecific competition can thus lead to an overestimation of the size of the coexistence regions. However, when the two competing species have relatively similar trait means and interspecific competition has a narrower competition width compared to intraspecific competition, an increase in variation can actually stabilize the coexistence between the competitors (Fig. S6.3). Furthermore, as with the earlier model, ITV in the two species affects the population dynamics in very similar ways, as evidenced by the symmetry in the subplots in Fig. 5 with respect to the line $\sigma_a = \sigma_b$. The exception to this pattern is the mirroring of the A wins and B wins scenarios: the species that wins is the species with the higher ITV (Fig. 5, second row).

3.2.2 Predator-prey model

In the predator-prey model, we assume trait variation to impact the attack rate ϕ in Eq. 4, such that $\phi = \overline{\gamma(a, b)}$. An increase in the attack rate ϕ favours invasion of the predator into the system, and coexistence is possible if (SI S7):

$$\phi > -\frac{r_B}{cK}. \tag{12}$$

Similar to the competition model, the qualitative effect of intraspecific trait variation on predator-prey coexistence can thus be determined solely based on whether it alters the value of ϕ such that it crosses the critical value in Eq. 12.

Here, we focus on the example of the logistic interaction function, where the interaction parameter only depends on the difference in trait values (Fig. 6). We consider four example scenarios

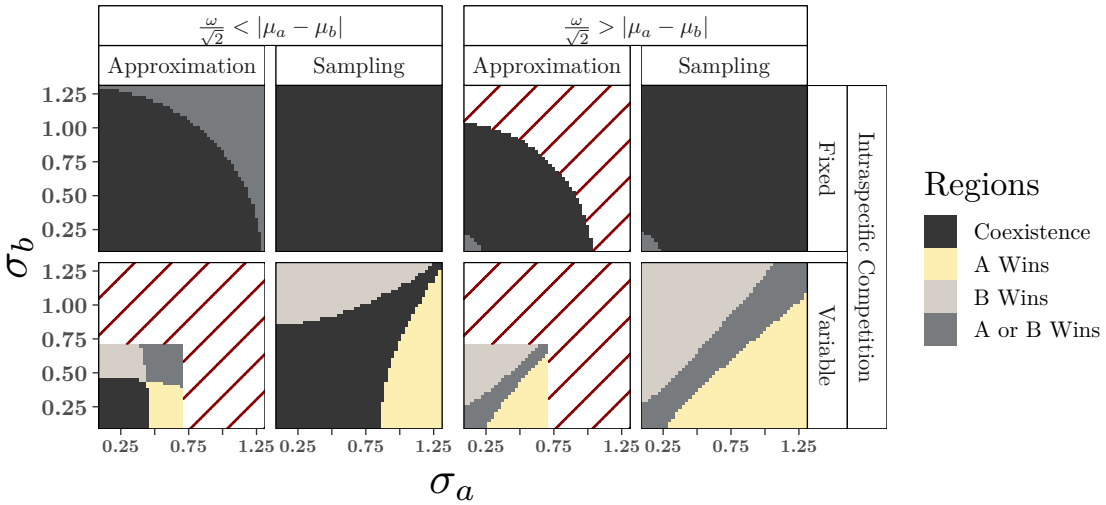

Figure 5 – Effect of ITV (σ_a and σ_b) on coexistence regions in the models with trait-independent (fixed) and trait-dependent (variable) intraspecific competition. In the red striped areas, the approximation predicts infeasible, negative competition coefficients. Fixed intraspecific competition implies $\alpha_{AA} = \alpha_{BB} = 1$ and only α_{AB} is affected by ITV. Variable intraspecific competition implies all αs (i.e. α_{AB}, α_{AA}, and α_{BB}) are ITV-dependent. For comparability between fixed and variable intraspecific competition, the maximum intraspecific competition coefficients ($c_{\max,AA}$ for species A and $c_{\max,BB}$ for species B) are fixed to 1. Furthermore, all the ωs (i.e. ω_{AB}, ω_{AA}, and ω_{BB}) are equal to 1. Other parameters: maximum interspecific interaction coefficient $c_{\max,AB} = 1.1$, $K_A = K_B = 500$, $\sigma_{a,b} = 0$, $|\mu_a - \mu_b| = 0.9$ for the panels on the left, and $|\mu_a - \mu_b| = 0.2$ for those on the right.

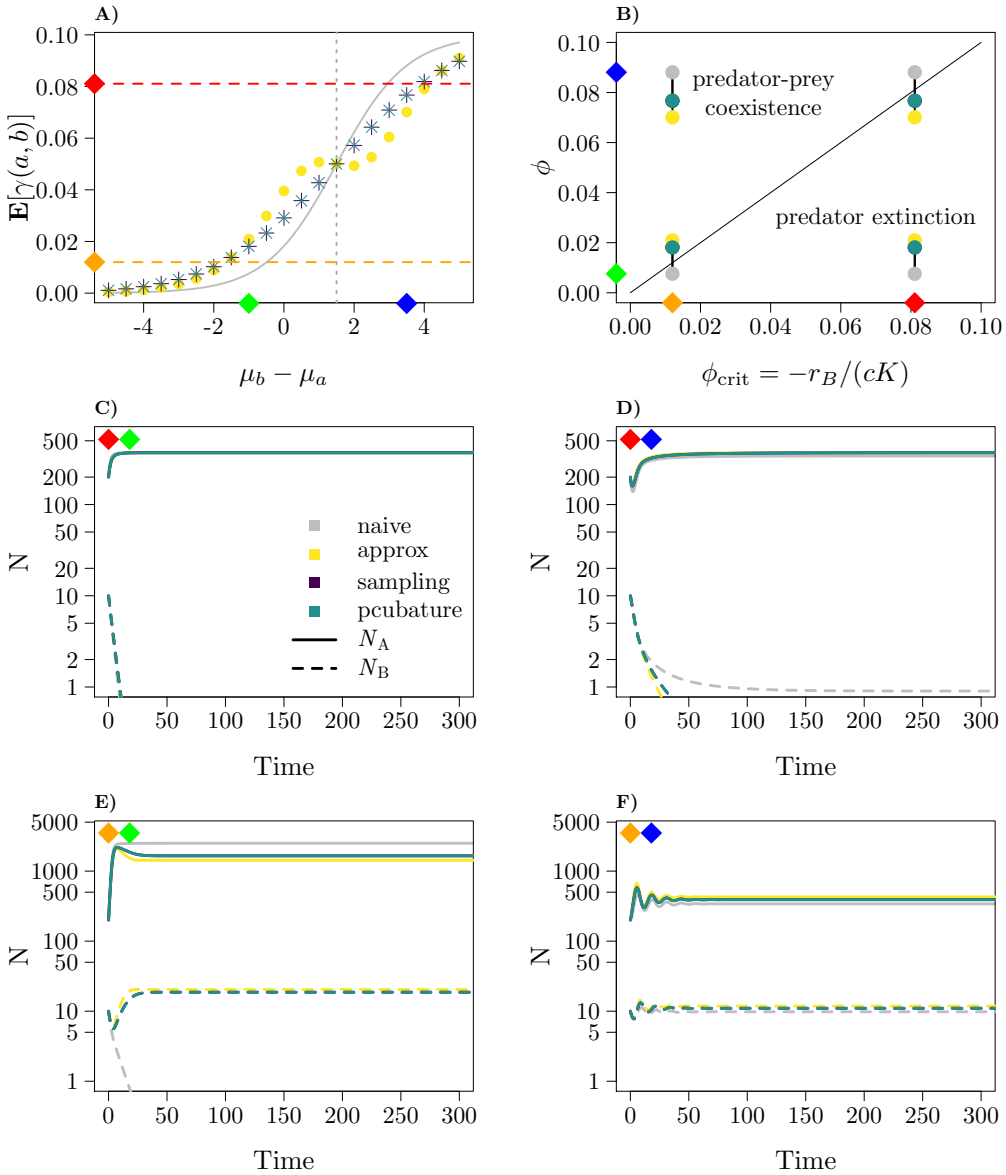

Figure 6 – Effects of intraspecific trait variation on the dynamics and qualitative outcome of the predator-prey model (Eq. 4). Here $\sigma_a = \sigma_b = 1.5, \sigma_{a,b} = 0$. A) Logistic interaction function with $p_{max} = 0.1, k = 1, h = 1.5$. B) Regions in parameter space with qualitatively different outcomes. C–F) Time series for four example parameter combinations. Red: $K = 370$, orange: $K = 2500$. Other parameter values for the predator-prey model: $r_A = 1, r_B = -0.3, c = 0.01$.

with different coexistence thresholds due to different carrying capacities (red and orange lines in Fig. 6A) and a predator-prey size difference below h (green diamonds) or above h (blue diamonds), where h is indicated by the dashed vertical line. Whether ITV can push the mean interaction across the coexistence threshold depends on the amount of ITV, the location of the threshold, and the difference between the trait value means. When the difference in mean trait values is below h (green), ITV increases ϕ, potentially up to above the critical coexistence threshold, if the threshold is low enough (orange case, but not red case), thereby promoting coexistence (Fig. 6A,B,E). If, on the other hand, the predator-prey size difference is above h (blue), ITV reduces the interaction coefficient. If the coexistence threshold is relatively high (red case), this can drive the predator to extinction even if without ITV both species could coexist (Fig. 6A,B,D). Even if the change in average interaction parameter is not large enough to change the qualitative outcome, the equilibrium population abundances can be affected (red-blue case, Fig. 6A,B,F). The equilibrium value of the prey abundance ($N_A^* = \frac{-r_B}{c\phi}$) decreases with increasing ϕ, while the equilibrium value of the predator ($N_B^* = \frac{r_A}{\phi}(1 + \frac{r_B}{c\phi K})$) first increases with ϕ and then decreases when the prey equilibrium value falls below $K/2$ (SI S7).

3.2.3 Density-dependent interaction function

So far we have focused on the case where the interaction function is independent of the densities of the species. However, when the number of interactions per time unit is limited for an individual of one of the species, the average response should saturate with their abundance. For example, there is an upper bound to the amount of prey that a predator can catch because the predator requires a certain amount of time to handle any caught prey item (handling time). The Rosenzweig-MacArthur model (Rosenzweig & MacArthur, 1963) explicitly takes this limitation into account. In SI S7.2, we study the case where the encounter rate is affected by variable predator and prey traits and we develop a numerical approach and an approximation to quantify the functional response and the resulting population dynamics. Similarly to the linear response predator-prey model with a logistic interaction function, the effect of trait variation on coexistence depended on the difference in mean trait value, with variation preventing predator extinction when the mean prey trait value

was slightly above the average predator trait value (Fig. S7.1a). In the density-dependent case, however, the effect is no longer symmetric and the reverse effect, when predators were relatively large, was much smaller.

The Taylor approximation was generally in good agreement with the "true" estimates. However, the Taylor approximation no longer provided clear direct insight into the effects of trait variation due to the complexities introduced by the nonlinear response function. On the other hand, the relatively quick calculation of the Taylor approximation weighs even stronger for this model where the average interaction function has to be reevaluated for many different values of N_A.

4 Discussion

Our results show how intraspecific trait variation in each of two interacting species can affect average competition coefficients and predation rates through two-dimensional nonlinear averaging. The magnitude and direction of this effect depend on the shape of the interaction function, average trait values, amounts of trait variation in each species, as well as on the trait covariance between interacting individuals. As a consequence, the joint population dynamics can be affected both quantitatively (e.g. influencing equilibrium population densities) and qualitatively (species coexistence or extinction).

Nonlinear averaging in 2D and the effect of ITV on interaction parameters

A highly accurate quantification of the nonlinear averaging effect in two dimensions requires a double integration over the interaction function with respect to the joint trait distribution or a Monte Carlo sampling scheme. In addition, when the amount of trait variation is relatively small, its effect on the average of the interaction function and thereby on the population dynamics can be approximated using an insightful and computationally less intensive Taylor approximation based on the curvatures of the interaction function.

The accuracy of our approximation depends on the joint trait distribution and interaction function. The approximation is exact if the interaction function is a second order polynomial. Otherwise,

the approximation is accurate when the curvatures are relatively constant over the part of trait-space where the bulk of the interactions take place. When this is not the case, the approximation may be inaccurate or even predict an effect in the opposite direction, as in our non-differentiable interaction function whenever interactions took place on both sides of a discontinuity (see Fig. $3e_2$). For the other interaction functions, the second order Taylor approximation always correctly predicted the direction of the change compared to the naive value (Fig. 3). However, in particular when variances were large, the approximation tended to overestimate their impact. The approximation thus correctly predicted whether an increase in variation promotes or hampers coexistence, but not always whether the amount of variation is sufficient to affect coexistence.

When trait variation can be described by a bivariate normal distribution, it is straightforward to include higher order terms in the approximation (as shown in SI S2.3). This improves the accuracy when trait variances are small, but decreases the accuracy when trait variances are large (Fig. S2.1). This behaviour is expected because, away from the point at which the approximation is performed, Taylor approximations do not necessarily converge with increasing number of terms (see for example §6.2.1 in Witelski & Bowen, 2015).

Taylor approximations have been used to link trait variation to population dynamics before, both in single-species models (Bjørnstad & Hansen, 1994) and in models with two or more species and one or more jointly distributed traits, each affecting a different ODE parameter (Hart *et al.*, 2016). More generally, such Taylor approximations have also been used to study the effect of spatio-temporal variation in environmental conditions on species' growth rates, as well as population and community dynamics (e.g. Gravel *et al.* 2011; Bernhardt *et al.* 2018; Denny 2019; and scale-transition theory by Chesson *et al.* 2005; Melbourne & Chesson 2005; Chesson 2012). In addition, quantifying the second derivative of an ecological response variable with respect to some trait value can be a short-cut to estimating the consequences of ITV in cases where experimentally manipulating the amount of ITV is not feasible (Inouye, 2005).

A complementary approach to quantifying the average interaction parameter that does not rely on a small variance approximation is to derive upper and lower bounds of the average interaction parameter $\overline{\gamma(a,b)}$. Rigorous theory in two dimensions exists for functions that are concave or convex

everywhere (Madansky, 1959; Ben-Tal & Hochman, 1972). Though promising, it is currently not clear whether such approaches can be extended to biologically realistic interaction functions with more complex shapes.

Competition model

ITV can affect coexistence in interspecific competition models through multiple pathways. Here we have focused on nonlinear averaging effects and a Gaussian interaction function where the competition strength is maximized if individuals have equal trait values. We found that when the trait means are far apart relative to the competition width, ITV increases interspecific competition, and when the trait means are close together, ITV decreases competition (Fig. $3c_2$, see also Barabás & D'Andrea 2016). This effect is similar to the interaction between phenotypic mismatch and trait variation in a single-species patch occupancy model (Gibert, 2016).

Although small-variance Taylor approximations have been used before to study the impacts of ITV on interspecific competition (e.g. Hart *et al.*, 2016), our two-dimensional approach adds additional insight and generality. In particular, when the strength of an interaction depends only on the difference in trait values between interacting individuals as assumed in most previous research, our approximation Eq. 8 shows that the variances in the two species have the same effect on the average interaction parameter. The effect of the covariance between the species on the average interaction parameter ranges from doubling the effect of the variances when species are perfectly negatively correlated to completely counteracting it when the two species are perfectly positively correlated. Only taking into account variation in one species could thus underestimate the effect of ITV by a factor of three, but also predict a nonzero effect of ITV that disappears when both species are studied. These quantitative differences translate into qualitative differences whenever they push the average interaction parameter across a coexistence threshold.

Our approach can also be applied to more general two-dimensional interaction functions where the effect of ITV differs between species. For example, for some parameterizations of the polynomial interaction function (Table 1), the curvatures in the a and b direction have the opposite sign and thus variation in one species can have the opposite effect as variation in the other. Thus ignoring

ITV in one of the species can lead to incorrect predictions for the direction of the effect of ITV.

Our approach further allows for trait variation affecting multiple ODE parameters simultaneously. Consistently with previous research (e.g. Hart *et al.*, 2016), our results show that when ITV affects inter- and intraspecific competition simultaneously the relative reduction in intraspecific competition tends to be larger compared to the relative decrease, or even increase, in interspecific competition, thereby hindering coexistence (SI S6.3). Interestingly, this finding is not general, as we have also detected cases where ITV effects on both intra- and interspecific competition can promote coexistence (Fig. S6.3).

Allowing variation to affect different ODE parameters simultaneously could also be used to include asymmetric competition. Specifically, one would have to define two different interaction functions, one for the effect of species A on species B and one for the reverse effect, and average each over the joint trait distribution separately to find their average values. In nature, asymmetric competition may have substantial consequences (Bassar *et al.*, 2017; Griffiths *et al.*, 2020), e.g. in above-ground competition in plant communities where large plants are expected to affect small plants much more than the other way around (Weiner, 1990). Our approach could similarly be extended to allow for multiple traits affecting different ODE parameters or systems with more than two species.

The effect of ITV on the strength and outcome of interspecific competition can also depend on population structure. In our model, such spatial structure can be encoded to some extent as covariance of the joint distribution function. For example, when covariance is negative, individuals tend to co-occur more with heterospecific individuals that are relatively dissimilar and thus in similarity-based competition the average strength of the competition is reduced (see Fig. $3d_4$). That spatial structure can profoundly shape the effects of ITV is also shown by Uriarte & Menge (2018). In their two-patch extension of the model by Hart *et al.* (2016), intraspecific variation can promote coexistence via nonlinear averaging if the overall inferior competitor is favored in the more productive patch, the opposite of what is found in the non-spatial model.

Overall, the effect of ITV on interspecific competition and ultimately on coexistence is context-dependent. Although we can thus not provide a general rule for the effect of ITV on coexistence

of two competitors, we can provide a more intuitive understanding for any given shape of the interaction function and species' trait distributions.

Predator-prey model

Variation in traits relevant for predator-prey interactions, such as prey susceptibility and predator selectivity, is commonly found in vertebrates (Pettorelli *et al.*, 2011). In our predator-prey model, coexistence between both species relies on the predators consuming enough prey to invade a system that contains only prey. Coexistence is therefore promoted whenever the average consumption parameter increases (SI S7). Similar to the competition model, whether trait variation changes coexistence qualitatively, depends on its quantitative effect on the average interaction parameter.

For the predator-prey model, our focus has mainly been on the logistic interaction function, where consumption increases as the predators increase in size relative to the prey. We found accordingly that the effect of ITV depends strongly on the magnitude and direction of the difference in trait means. If we had instead used the Gaussian interaction function in the predator-prey model, the direction of the difference in trait values would be irrelevant for the average consumption and coexistence would only depend on the magnitude of phenotypic mismatch and the amount of trait variation. Such a mismatch-based interaction function has been used for example in a Rosenzweig-MacArthur model where an increase in variation in attack rate and handling time tends to be stabilizing and increase coexistence when trait mismatch is large (Gibert & DeLong, 2015; Gibert & Brassil, 2014).

Depending on the interaction function, the average consumption parameter can also be affected by indirect effects through the covariance, as emphasized by our analysis of a non-differentiable interaction function. Here, an increase in predator trait variation under constant correlation led to an increased covariance between prey and predator traits and thereby the average consumption (Fig. $3e_4$). Such an indirect effect of variation could never be observed when only focusing on a single species. Furthermore, as with the competition model, an interaction function with curvatures of opposite signs is also conceivable for the predator-prey model. As a consequence, the effect of variation in one species could be negated or even reversed by variation in the partner species. For a

full understanding, it is therefore vital to take into account variation in both species simultaneously.

In the main text, we have focused on a predator-prey model where the amount of consumed prey scales linearly with the total prey abundance. Biologically, it is more realistic for the total consumption rate to respond nonlinearly to prey density, such that it is limited by the density-dependent prey search time when prey are scarce, and by the constant handling time when prey are abundant. This can be achieved, for example, by explicitly keeping track of the number of hunting and the number of handling predators separately (Okuyama, 2012), or by introducing a type II functional response, as in the Rosenzweig-MacArthur model. Here, we explored the effect of trait-variation in such a Rosenzweig-MacArthur model when used with a logistic interaction function in two dimensions (SI S7.2). In this case, the projected population dynamics depend on the method for averaging the consumption rate: one can either average the total rate (as done by Okuyama, 2008), or average the numerator and denominator separately (our approach). Conceptually, the former method describes the case where any given predator only encounters one type of prey item, while our method corresponds to each predator encountering the full distribution of prey items. Note that we cannot calculate a single average interaction parameter, because the estimate of $\overline{\gamma(a,b)}$ depends on the amount of prey and is thus time-dependent. We find that due to the nonlinear response, the effect of trait variation on the average predation rate is no longer symmetric around the line $b - a = h$, and instead the effect of trait variation is relatively small when the mean trait values predict nearly saturated predators.

More generally, the total interaction parameter cannot necessarily always be written as the sum of independent individual-by-individual interactions. For example, in plant communities, so-called associational effects are often observed where the herbivory pressure on a focal plant depends on its neighbours and their traits, e.g. their level of defense or ontogenetic stage (Hahn & Orrock, 2016; Cope *et al.*, 2020). These effects are thought to be mediated by herbivore foraging behaviour. Furthermore, individuals may adjust their physiology or behaviour in response to an interaction partner, which then affects the outcome of subsequent interactions with other individuals (e.g. physiological tracking of herbivores, Pearse *et al.*, 2018).

Outlook

Throughout the manuscript, we have assumed static non-heritable trait distributions, as have many previous studies (e.g. Begon & Wall, 1987). Such static trait distributions can for example arise through stable age or stage structures (as expected in matrix models and IPMs, see for example Easterling *et al.*, 2000; Caswell, 2001; Ellner *et al.*, 2016) or because of phenotypic plasticity in response to a distribution of microenvironments (Moran *et al.*, 2016). However, one would expect the trait distributions to change both directly as well as over multiple generations for example if prey with certain trait values are being consumed more frequently, or individuals with a certain trait value face stronger competition than others. To allow for changing trait distributions over time, we could combine our two-dimensional nonlinear averaging framework with one of the existing approaches for modeling changes in trait distributions. For example, assuming asexual reproduction with perfect heritability, we could use partial differential equations to model the eco-evolutionary dynamics of population sizes and trait distributions (see e.g. Senthilnathan & Gavrilets, 2021). For systems where heritability is not perfect, but the prey can be described in terms of two genetic types with different trait means and remaining plastic trait variation in each type (see e.g. Schreiber *et al.*, 2011; Okuyama, 2011), we can average the interaction between each of the prey types and the predator and still obtain an intuitive understanding of the effect of ITV on the average interaction parameters. Alternatively, we could allow for temporarily changing trait values in either species by calculating a selection gradient from the interaction function and letting the mean trait value evolve accordingly (e.g. Barabás & D'Andrea, 2016; Bengfort *et al.*, 2017). At any given time step we can then calculate the effect of ITV on the average interaction function, based on the mean trait values, and we can use the approximation to speed up the process.

As an alternative to fully modelling the trait dynamics, for some interaction functions, it may be possible to find a stable evolutionary endpoint. For example, in the competition model we would expect that the system will try to lower overall competition and therefore evolve to the point where α_{AB} is minimal, which can be achieved by having the two trait mean values evolve away from each other. If such a stable state can be identified, the methods we used can predict the effect of any

remaining plastic or demographic (e.g. due to age) trait variation on the population dynamics at that stable state.

The models we use mainly concern ecological dynamics and therefore lead to predictions that can be tested over relatively short time scales. In particular we want to highlight two examples for testable predictions. Firstly, for interactions that only depend on a trait difference, we have predicted that the average interaction value should depend equally strongly on variation in each of the species, while positive across-species trait correlations may diminish the effect of ITV. Secondly, we have shown that trait variation can enhance coexistence of competing species when the species are similar and intraspecific competition is less trait-dependent than interspecific competition.

Conclusion

Our approach allows for a straightforward and rapid assessment of the expected effect of variation in two species, both on the average interaction parameter, as well as the population dynamics, and these effects could directly be estimated from the shape of the interaction function. In particular, we have shown that although there are few general rules regarding the direction and magnitude of the effect of ITV on population dynamics, it is nearly always crucial to take into account variation in both species simultaneously. Even in the absence of evolution, variation among interacting individuals can make or break the coexistence between species.

Author contributions:

KJvB and MJW designed the approach and led the writing of the manuscript. KJvB led the analyses. All authors contributed code for the analyses, and contributed at least one subsection for the initial draft. All authors contributed to revisions.

Acknowledgements

This work was supported by the German Research foundation DFG (project numbers 316099922 and 396782288 within SFB TRR 212 and WI 4544/2-1 within FOR 3000).

Supporting information

S1–S7 additional analyses and results.

References

Banitz, T. (2019) Spatially structured intraspecific trait variation can foster biodiversity in disturbed, heterogeneous environments. *Oikos* **128**, 1478–1491.

Barabás, G. & D'Andrea, R. (2016) The effect of intraspecific variation and heritability on community pattern and robustness. *Ecology Letters* **19**, 977–986.

Bartomeus, I., Gravel, D., Tylianakis, J.M., Aizen, M.A., Dickie, I.A. & Bernard-Verdier, M. (2016) A common framework for identifying linkage rules across different types of interactions. *Functional Ecology* **30**, 1894–1903.

Bassar, R.D., Travis, J. & Coulson, T. (2017) Predicting coexistence in species with continuous ontogenetic niche shifts and competitive asymmetry. *Ecology* **98**, 2823–2836.

Begon, M., Townsend, C.R. & Harper, J.L. (2006) *Ecology - From Individuals to Ecosystems*. Blackwell Publishing Ltd, Oxford, UK, 4th edn.

Begon, M. & Wall, R. (1987) Individual variation and competitor coexistence: a model. *Functional Ecology* **1**, 237–241.

Ben-Tal, A. & Hochman, E. (1972) More bounds on the expectation of a convex function of a random variable. *Journal of Applied Probability* **9**, 803–812.

Bengfort, M., van Velzen, E. & Gaedke, U. (2017) Slight phenotypic variation in predators and prey causes complex predator-prey oscillations. *Ecological Complexity* **31**, 115–124.

Bernhardt, J.R., Sunday, J.M., Thompson, P.L. & O'Connor, M.I. (2018) Nonlinear averaging of thermal experience predicts population growth rates in a thermally variable environment. *Proceedings of the Royal Society B: Biological Sciences* **285**, 20181076.

Bjørnstad, O.N. & Hansen, T.F. (1994) Individual variation and population dynamics. *Oikos* **69**, 167–171.

Bolnick, D.I., Amarasekare, P., Araújo, M.S., Bürger, R., Levine, J.M., Novak, M., Rudolf, V.H., Schreiber, S.J., Urban, M.C. & Vasseur, D.A. (2011) Why intraspecific trait variation matters in community ecology. *Trends in Ecology & Evolution* **26**, 183–192.

Caswell, H. (2001) *Matrix Population Models: construction, analysis and interpretation.* Sinauer Associates, Inc. Publishers, Sunderland, MA, USA, 2nd edn.

Chesson, P. (2012) Scale transition theory: Its aims, motivations and predictions. *Ecological Complexity* **10**, 52–68.

Chesson, P., Donahue, M.J., Melbourne, B.A. & Sears, A.L.W. (2005) Scale transition theory for understanding mechanisms in metacommunities. *Metacommunities: Spatial Dynamics and Ecological Communities* (eds. M. Holyoak, M.A. Leibold & R.D. Holt), pp. 279–306, The University of Chicago Press, Chicago, IL, USA.

Cope, O.L., Becker, Z., Ode, P.J., Paul, R.L. & Pearse, I.S. (2020) Associational effects of plant ontogeny on damage by a specialist insect herbivore. *Oecologia* **193**, 593–602.

Denny, M. (2019) Performance in a variable world: using Jensen's inequality to scale up from individuals to populations. *Conservation Physiology* **7**, coz053.

Des Roches, S., Post, D.M., Turley, N.E., Bailey, J.K., Hendry, A.P., Kinnison, M.T., Schweitzer, J.A. & Palkovacs, E.P. (2018) The ecological importance of intraspecific variation. *Nature Ecology & Evolution* **2**, 57–64.

Easterling, M.R., Ellner, S.P. & Dixon, P.M. (2000) Size-specific sensitivity: applying a new structured population model. *Ecology* **81**, 694–708.

Ellner, S.P., Childs, D.Z. & Rees, M. (2016) *Data-driven Modelling of Structured Populations: A Practical Guide to the Integral Projection Model*. Springer International Publishing, Cham, CH.

Genung, M.A., Bailey, J.K. & Schweitzer, J.A. (2012) Welcome to the neighbourhood: interspecific genotype by genotype interactions in *Solidago* influence above- and belowground biomass and associated communities. *Ecology Letters* **15**, 65–73.

Gibert, J.P. (2016) The effect of phenotypic variation on metapopulation persistence. *Population Ecology* **58**, 345–355.

Gibert, J.P. & Brassil, C.E. (2014) Individual phenotypic variation reduces interaction strengths in a consumer-resource system. *Ecology and Evolution* **4**, 3703–3713.

Gibert, J.P. & DeLong, J.P. (2015) Individual variation decreases interference competition but increases species persistence. *Advances in Ecological Research: Trait-Based Ecology - From Structure to Function* (eds. S. Pawar, G. Woodward & A.I. Dell), vol. 52, pp. 45–64, Elsevier Ltd., Waltham, MA ,USA, 1st edn.

Gravel, D., Guichard, F. & Hochberg, M.E. (2011) Species coexistence in a variable world. *Ecology Letters* **14**, 828–839.

Griffiths, J.I., Childs, D.Z., Bassar, R.D., Coulson, T., Reznick, D.N. & Rees, M. (2020) Individual differences determine the strength of ecological interactions. *Proceedings of the National Academy of Sciences* **117**, 17068–17073.

Hahn, P.G. & Orrock, J.L. (2016) Neighbor palatability generates associational effects by altering herbivore foraging behavior. *Ecology* **97**, 2103–2111.

Hart, S.P., Schreiber, S.J. & Levine, J.M. (2016) How variation between individuals affects species coexistence. *Ecology Letters* **19**, 825–838.

Hausch, S., Vamosi, S.M. & Fox, J.W. (2018) Effects of intraspecific phenotypic variation on species coexistence. *Ecology* **99**, 1453–1462.

Inouye, B.D. (2005) The importance of the variance around the mean effect size of ecological processes: Comment. *Ecology* **86**, 262–265.

Isserlis, L. (1918) On a formula for the product-moment coefficient of any order of a normal frequency distribution in any number of variables. *Biometrika* **12**, 134–139.

Jensen, J.L.W.V. (1905) Sur les fonctions convexes et les inégalités entre les valeurs moyennes. *Acta Mathematica* **30**, 175–193.

Madansky, A. (1959) Bounds on the expectation of a convex function of a multivariate random variable. *The Annals of Mathematical Statistics* **30**, 743–746.

Maynard, D.S., Serván, C.A., Capitán, J.A. & Allesina, S. (2019) Phenotypic variability promotes diversity and stability in competitive communities. *Ecology Letters* **22**, 1776–1786.

Melbourne, B.A. & Chesson, P. (2005) Scaling up population dynamics: integrating theory and data. *Oecologia* **145**, 179–187.

Moran, E.V., Hartig, F. & Bell, D.M. (2016) Intraspecific trait variation across scales: implications for understanding global change responses. *Global Change Biology* **22**, 137–150.

Moran, N.P., Caspers, B., Chakarov, N., Ernst, U., Fricke, C., Kurtz, J., Lilie, N.D., Lo, L.K., Müller, C., Takola, E., Trimmer, P.C., van Benthem, K.J., R, R., Winternitz, J. & Wittmann, M.J. (2020) Shifts between cooperation and antagonism driven by individual variation: A systematic synthesis review. *preprint at EcoEvoRxiv, doi:10.32942/osf.io/sbrvu* .

Narasimhan, B., Johnson, S.G., Hahn, T., Bouvier, A. & Kiêu, K. (2019) *cubature: Adaptive Multivariate Integration over Hypercubes*. R package version 2.0.4.

Okuyama, T. (2008) Individual behavioral variation in predator–prey models. *Ecological Research* **23**, 665–671.

Okuyama, T. (2011) Individual variation in prey choice in a predator-prey community. *Theoretical Population Biology* **79**, 64–69.

Okuyama, T. (2012) Behavioral states of predators stabilize predator-prey dynamics. *Theoretical Ecology* **5**, 605–610.

Pearse, I.S., Paul, R. & Ode, P.J. (2018) Variation in plant defense suppresses herbivore performance. *Current Biology* **28**, 1981–1986.e2.

Pettorelli, N., Coulson, T., Durant, S.M. & Gaillard, J.M. (2011) Predation, individual variability and vertebrate population dynamics. *Oecologia* **167**, 305–314.

Phillips, B.L., Brown, G.P. & Shine, R. (2003) Assessing the potential impact of cane toads on Australian snakes. *Conservation Biology* **17**, 1738–1747.

Phillips, B.L. & Shine, R. (2004) Adapting to an invasive species: toxic cane toads induce morphological change in Australian snakes. *Proceedings of the National Academy of Sciences of the United States of America* **101**, 17150–17155.

Rosenzweig, M.L. & MacArthur, R.H. (1963) Graphical representation and stability conditions of predator-prey interactions. *The American Naturalist* **97**, 209–223.

Ruel, J.J. & Ayres, M.P. (1999) Jensen's inequality predicts effects of environmental variation. *Trends in Ecology & Evolution* **14**, 361–366.

Schirmer, A., Hoffmann, J., Eccard, J.A. & Dammhahn, M. (2020) My niche: individual spatial niche specialization affects within- and between-species interactions. *Proceedings of the Royal Society B: Biological Sciences* **287**, 20192211.

Schreiber, S.J., Bürger, R. & Bolnick, D.I. (2011) The community effects of phenotypic and genetic variation within a predator population. *Ecology* **92**, 1582–1593.

Senthilnathan, A. & Gavrilets, S. (2021) Ecological consequences of intraspecific variation in co-evolutionary systems. *The American Naturalist* **197**, 1–17.

Uriarte, M. & Menge, D. (2018) Variation between individuals fosters regional species coexistence. *Ecology Letters* **21**, 1496–1504.

Violle, C., Enquist, B.J., McGill, B.J., Jiang, L., Albert, C.H., Hulshof, C., Jung, V. & Messier, J. (2012) The return of the variance: intraspecific variability in community ecology. *Trends in Ecology & Evolution* **27**, 244–252.

Weiner, J. (1990) Asymmetric competition in plant populations. *Trends in Ecology & Evolution* **5**, 360–364.

Witelski, T. & Bowen, M. (2015) *Methods of mathematical modelling: continuous systems and differential equations*. Springer International Publishing, Cham, CH.

S1 Shifting non-independence to the interaction function

Any non-independence in the joint distribution can also be accounted for instead in the interaction function since

$$\iint \gamma(a,b) f_{AB}(a,b) \mathrm{d}a\mathrm{d}b = \iint \gamma^*(a,b) f_A(a) f_B(b) \mathrm{d}a\mathrm{d}b \tag{S1.1}$$

with a new interaction function

$$\gamma^*(a,b) = \frac{\gamma(a,b) f_{AB}(a,b)}{f_A(a) f_B(b)} \tag{S1.2}$$

and marginal trait distributions $f_A(a)$ and $f_B(b)$.

S2 Derivation of the approximation

S2.1 Up to second order

For a two-dimensional function $\gamma(a, b)$, up to second order, the Taylor approximation around the point $(\overline{a}, \overline{b})$ is:

$$\gamma(a,b) \approx \gamma(\overline{a},\overline{b}) + (a-\overline{a}) \left.\frac{\partial \gamma}{\partial a}\right|_{(\overline{a},\overline{b})} + (b-\overline{b}) \left.\frac{\partial \gamma}{\partial b}\right|_{(\overline{a},\overline{b})} + \tag{S2.1}$$

$$\frac{1}{2}\left((a-\overline{a})^2 \left.\frac{\partial^2 \gamma}{\partial a^2}\right|_{(\overline{a},\overline{b})} + (b-\overline{b})^2 \left.\frac{\partial^2 \gamma}{\partial b^2}\right|_{(\overline{a},\overline{b})} + 2(a-\overline{a})(b-\overline{b}) \left.\frac{\partial^2 \gamma}{\partial a \partial b}\right|_{(\overline{a},\overline{b})}\right). \tag{S2.2}$$

Taking the expectation over the joint distribution of a and b yields

$$\overline{\gamma(a,b)} = \mathbf{E}[\gamma(a,b)] \approx \mathbf{E}\left[\gamma(\overline{a},\overline{b}) + (a_i-\overline{a}) \left.\frac{\partial \gamma}{\partial a}\right|_{(\overline{a},\overline{b})} + (b_i-\overline{b}) \left.\frac{\partial \gamma}{\partial b}\right|_{(\overline{a},\overline{b})} + \right. \tag{S2.3}$$

$$\left. \frac{1}{2}\left((a_i-\overline{a})^2 \left.\frac{\partial^2 \gamma}{\partial a^2}\right|_{(\overline{a},\overline{b})} + (b_i-\overline{b})^2 \left.\frac{\partial^2 \gamma}{\partial b^2}\right|_{(\overline{a},\overline{b})} + 2(a_i-\overline{a})(b_i-\overline{b}) \left.\frac{\partial^2 \gamma}{\partial a \partial b}\right|_{(\overline{a},\overline{b})}\right)\right]. \tag{S2.4}$$

We can take the expectation for each term independently. Furthermore, the partial derivatives can be taken in front of the sum, since these are always approximated at the same point and do not depend on a and b. Finally, we realize that:

$$\mathbf{E}[(a-\overline{a})] = 0 \tag{S2.5}$$

$$\mathbf{E}[(a-\overline{a})^2] = \sigma_a^2 \tag{S2.6}$$

$$\mathbf{E}[(a-\overline{a})(b-\overline{b})] = \sigma_{a,b}, \tag{S2.7}$$

to find that:

$$\overline{\gamma(a,b)} \approx \gamma(\overline{a},\overline{b}) + \frac{1}{2}\sigma_a^2 \left.\frac{\partial^2 \gamma}{\partial a^2}\right|_{(\overline{a},\overline{b})} + \frac{1}{2}\sigma_b^2 \left.\frac{\partial^2 \gamma}{\partial b^2}\right|_{(\overline{a},\overline{b})} + \sigma_{a,b} \left.\frac{\partial^2 \gamma}{\partial a \partial b}\right|_{(\overline{a},\overline{b})}. \tag{S2.8}$$

S2.2 Third order approximation for the multivariate normal distribution

In this section we will extend the approximation to higher order for cases where a and b are generated by a bivariate normal distribution. According to Isserlis' theorem (Isserlis, 1918), in this case the third order central moments should all be zero and hence third-order derivatives do not contribute to an approximation of $\overline{\gamma(a,b)}$. For traits that are distributed according to a bivariate normal distribution our second order approximation is therefore actually valid up to third order.

S2.3 Higher order approximations

Using Isserlis' theorem it is possible to calculate higher-order approximations as well for traits that are distributed according to a bivariate normal distribution.

$$\gamma(a,b) \approx \gamma(\overline{a},\overline{b}) + \sum_{d=1}^{\kappa} \left(\frac{1}{d!} \sum_{a_n=0}^{d} \binom{d}{a_n} (a-\overline{a})^{a_n} (b-\overline{b})^{d-a_n} \left. \frac{\partial^d \gamma}{\partial a^{a_n} \partial b^{d-a_n}} \right|_{\overline{a},\overline{b}} \right). \tag{S2.9}$$

With a and b coming from a bivariate normal distribution, we can write:

$$\overline{\gamma(a,b)} \approx \gamma(\overline{a},\overline{b}) + \sum_{d=1}^{\kappa} \left(\frac{1}{d!} \sum_{a_n=0}^{d} \binom{d}{a_n} \mathbf{E}[(a-\overline{a})^{a_n} (b-\overline{b})^{d-a_n}] \left. \frac{\partial^d \gamma}{\partial a^{a_n} \partial b^{d-a_n}} \right|_{\overline{a},\overline{b}} \right). \tag{S2.10}$$

Isserlis' theorem allows us to calculate $\mathbf{E}[(a-\overline{a})^{a_n}(b-\overline{b})^{d-a_n}]$ for bivariate normal distributions. Specifically, it states that $\mathbf{E}[(a-\overline{a})^{a_n}(b-\overline{b})^{d-a_n}] = 0$ whenever d is odd. For the even cases, it states:

$$\mathbf{E}[(a-\overline{a})^{a_n}(b-\overline{b})^{d-a_n}] = \sum \sigma_a^{2^x} \sigma_b^{2^y} \sigma_{a,b}^z. \tag{S2.11}$$

The sum is taken over all possible ways of partitioning a set of a_n $a-\overline{a}$ items and $d-a_n$ $b-\overline{b}$ items into $\frac{d}{2}$ pairs. For each partition, x corresponds to the number $a-\overline{a}$,$a-\overline{a}$ pairs it contains, y to the number of $b-\overline{b}$,$b-\overline{b}$ pairs it contains and z to the number of $a-\overline{a}$,$b-\overline{b}$ pairs. Importantly $\frac{d}{2} = x+y+z$. Given a_n, the number of pairs of each type is fully specified by the number of mixed pairs, i.e. $x = \frac{1}{2}(a_n - z)$ and $y = \frac{d-a_n-z}{2}$. Thus the sum can be formulated to run over 1 dimension

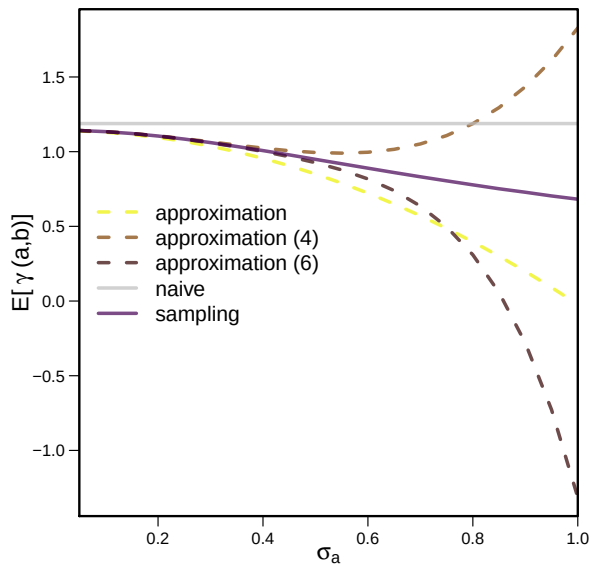

Figure S2.1 – Estimates of γ using the Gaussian interaction function with $c_{max} = 1.2$, $\omega = 1$, $\mu_a = 0$, $\mu_b = 0.1$, $\rho_{a,b} = 0$, $\sigma_b = 0.2$.

only:

$$\mathbf{E}[(a-\overline{a})^{a_n}(b-\overline{b})^{d-a_n}] = \sum_{z=z_0}^{\min(a_n,d-a_n)} N_z \sigma_a^{2\,\frac{1}{2}(a_n-z)} \sigma_b^{2\,\frac{1}{2}(d-a_n-z)} \sigma_{a,b}^{z}, \tag{S2.12}$$

with

$$z_0 = \begin{cases} 0 & \text{if } a_n \text{ is even} \\ 1 & \text{if } a_n \text{ is odd} \end{cases} \tag{S2.13}$$

and N_z the number of partitions with z mixed $a-\overline{a}$, $b-\overline{b}$ pairs.

The accuracy of the higher order approximations for a Gaussian interaction function depends on the amount of variation in σ_a (Fig. S2.1). This figure shows that the sixth and fourth order approximations are closer to the sampled, true, values when σ_a is small than the standard second order approximation. However, as the amount of variation increases, the higher order approximations diverge more strongly from the true values, until they become even less accurate than the naive values. Additionally, note that the the direction of the divergence is inverted from one approximation to the next higher even order.

S3 Covariance and the direction of the effect of ITV on the average interaction value for the polynomial interaction function

Here we consider the case where p_1 and p_2 in the polynomial interaction function have the same sign. If both are positive and $\sigma_{a,b} = 0$, intraspecific variation in either species always has a positive effect. The analogous result is true if both p_1 and p_2 are negative. Here we explore under what conditions the direction of the effect holds even with a non-zero covariance and under what conditions a non-zero covariance can change the direction of the effect.

Assume that $p_1, p_2 > 0$. Then, to find conditions for p_3 such that the effect of ITV will be positive irrespective of the parameters of the joint distribution, we are looking for the values of p_3 such that

$$p_1\sigma_a^2 + p_2\sigma_b^2 + p_3\sigma_{a,b} > 0 \tag{S3.1}$$

for all possible bivariate distributions. We rewrite this as:

$$(\sqrt{p_1}\sigma_a - \sqrt{p_2}\sigma_b)^2 + 2\sqrt{p_1}\sqrt{p_2}\sigma_a\sigma_b + p_3\sigma_{a,b} > 0. \tag{S3.2}$$

Since the mimimum value of the first term for any joint distribution is zero, we need the second term to be positive:

$$p_3\sigma_{a,b} + 2\sqrt{p_1}\sqrt{p_2}\sigma_a\sigma_b > 0 \tag{S3.3}$$

$$-p_3\frac{\sigma_{a,b}}{\sigma_a\sigma_b} < 2\sqrt{p_1}\sqrt{p_2}. \tag{S3.4}$$

By the Cauchy-Schwarz inequality, $-\sigma_a\sigma_b \leq \sigma_{a,b} \leq \sigma_a\sigma_b$ and thus the term on the left ranges between p_3 and $-p_3$. The condition must hold over this whole range, and therefore we must have $|p_3| < 2\sqrt{p_1}\sqrt{p_2}$ so that the effect of intraspecific trait variation is always positive. Analogously if $p_1, p_2 < 0$, the effect of intraspecific trait variation is always negative if $|p_3| < 2\sqrt{-p_1}\sqrt{-p_2}$, which

is the case for example in Fig. 3b.

S4 Approximation when γ only depends on the difference in trait value

A special case emerges when $\gamma(a, b)$ only depends on the different between a and b and hence can be written as $\gamma(u(a, b))$, with $u(a, b) = a - b$. Using the chain rule, we can find the first order partial derivatives for γ:

$$\frac{\partial \gamma}{\partial a} = \frac{\partial \gamma}{\partial u}\frac{\partial u}{\partial a} \tag{S4.1}$$

$$\frac{\partial \gamma}{\partial b} = \frac{\partial \gamma}{\partial u}\frac{\partial u}{\partial b}, \tag{S4.2}$$

given the definition of u, this becomes:

$$\frac{\partial \gamma}{\partial a} = \frac{\partial \gamma}{\partial u} \tag{S4.3}$$

$$\frac{\partial \gamma}{\partial b} = -\frac{\partial \gamma}{\partial u}. \tag{S4.4}$$

Hence, in this case we find that $\frac{\partial \gamma}{\partial a} = -\frac{\partial \gamma}{\partial b}$. We proceed to calculate the second order derivatives, where we use the symmetry of derivatives ($\frac{\partial}{\partial x}\left(\frac{\partial f}{\partial y}\right) = \frac{\partial}{\partial y}\left(\frac{\partial f}{\partial x}\right)$) and Eq. S4.3–S4.4:

$$\frac{\partial^2 \gamma}{\partial a^2} = \frac{\partial}{\partial a}\left(\frac{\partial \gamma}{\partial u}\right) = \frac{\partial}{\partial u}\left(\frac{\partial \gamma}{\partial a}\right) = \frac{\partial}{\partial u}\left(\frac{\partial \gamma}{\partial u}\right) \tag{S4.5}$$

$$\frac{\partial^2 \gamma}{\partial b^2} = -\frac{\partial}{\partial b}\left(\frac{\partial \gamma}{\partial u}\right) = -\frac{\partial}{\partial u}\left(\frac{\partial \gamma}{\partial b}\right) = \frac{\partial}{\partial u}\left(\frac{\partial \gamma}{\partial u}\right) \tag{S4.6}$$

$$\frac{\partial^2 \gamma}{\partial a \partial b} = \frac{\partial}{\partial b}\left(\frac{\partial \gamma}{\partial u}\right) = \frac{\partial}{\partial u}\left(\frac{\partial \gamma}{\partial b}\right) = -\frac{\partial}{\partial u}\left(\frac{\partial \gamma}{\partial u}\right). \tag{S4.7}$$

This result shows that when $\gamma(a, b)$ only depends on the difference between a and b,

$$\frac{\partial^2 \gamma}{\partial a^2} = \frac{\partial^2 \gamma}{\partial b^2} = -\frac{\partial^2 \gamma}{\partial a \partial b}. \tag{S4.8}$$

We can use this identity to simplify the approximation of $\overline{\gamma(a,b)}$ from Eq. 2:

$$\overline{\gamma(a,b)} \approx \gamma(\overline{a},\overline{b}) + \left.\frac{\partial^2\gamma}{\partial a^2}\right|_{(\overline{a},\overline{b})} \left(\frac{1}{2}\sigma_a^2 + \frac{1}{2}\sigma_b^2 - \sigma_{a,b}\right). \tag{S4.9}$$

Hence, an increase in variance in a has the exact same effect as an increase in variance in b. Furthermore, increasing covariance between a and b acts opposed to the direct effect of the variances. However, by the Cauchy-Schwarz inequality, $|\sigma_{a,b}| \leq \sigma_a\sigma_b$ and thus

$$\left(\frac{1}{2}\sigma_a^2 + \frac{1}{2}\sigma_b^2 - \sigma_{a,b}\right) \geq \frac{1}{2}\left(\sigma_a^2 - 2\sigma_a\sigma_b + \sigma_b^2\right) = \frac{1}{2}\left(\sigma_a - \sigma_b\right)^2 \geq 0. \tag{S4.10}$$

Hence the covariance term can never change the sign of the overall effect. In the special case when a and b have the same variance and they are perfectly correlated ($\rho_{a,b} = 1 \rightarrow \sigma_{a,b} = \sigma_a\sigma_b$), the term on the right cancels out and the expression can be simplified to:

$$\overline{\gamma(a,b)} \approx \gamma(\overline{a},\overline{b}). \tag{S4.11}$$

S5 Deriving lines of zero and maximal curvature for the Gaussian and the logistic interaction function

S5.1 Gaussian interaction function

All curvatures of the Gaussian interaction function (see Table 1) vanish when:

$$\frac{4(a-b)^2 - 2\omega^2}{\omega^4}\gamma(a,b) = 0. \tag{S5.1}$$

This occurs when either $\gamma(a,b) = 0$, and hence when the difference between a and b goes to infinity, or when:

$$4(a-b)^2 - 2\omega^2 = 0, \tag{S5.2}$$

or:

$$a - b = \pm \frac{\omega}{\sqrt{2}}. \tag{S5.3}$$

The effect of variation is the strongest (at least for small variance and in the approximation) when the curvature reaches an extreme value. In the a direction, this occurs when:

$$\frac{\partial^3 \gamma(a,b)}{\partial a^3} = 0, \tag{S5.4}$$

or:

$$\frac{\partial}{\partial a}\left(\frac{4(a-b)^2 - 2\omega^2}{\omega^4}\gamma(a,b)\right) = 0, \tag{S5.5}$$

which is equal to:

$$\left(\frac{4(a-b)^2 - 2\omega^2}{\omega^4}\right)\frac{\partial \gamma(a,b)}{\partial a} + \gamma(a,b)\frac{\partial}{\partial a}\left(\frac{4(a-b)^2 - 2\omega^2}{\omega^4}\right) = 0. \tag{S5.6}$$

This expression can be simplified to:

$$\gamma(a,b)(a-b)\left(\frac{4(a-b)^2 - 2\omega^2}{\omega^4}(\frac{-2}{\omega^2}) + \frac{8}{\omega^4}\right) = 0. \tag{S5.7}$$

This occurs when either $\gamma(a,b) = 0$ (when the absolute difference between a and b goes to infinity), when $a = b$ and when:

$$\frac{4(a-b)^2}{\omega^4} = \frac{6}{\omega^2}. \tag{S5.8}$$

or:

$$(a-b)^2 = 1.5\omega^2, \tag{S5.9}$$

or:

$$a - b = \pm\sqrt{3}\frac{\omega}{\sqrt{2}}. \tag{S5.10}$$

The earlier found line at $a = b$ corresponds to a line of minimal (negative) curvature, while this second line (Eq. S5.10) corresponds to a line of maximal curvature.

S5.2 Logistic interaction function

For the logistic interaction function

$$\gamma(a,b) = p_{\max}\frac{1}{1+e^{-k(b-a-h)}}, \tag{S5.11}$$

all curvatures (see Table 1) vanish when:

$$k^2\left(\gamma(a,b) + \frac{2\gamma(a,b)^3}{p_{\max}^2} - 3\frac{\gamma(a,b)^2}{p_{\max}}\right) = 0. \tag{S5.12}$$

With $k \neq 0$, this occurs when:

$$\gamma(a,b)\left(1 + \frac{2\gamma(a,b)^2}{p_{\max}^2} - 3\frac{\gamma(a,b)}{p_{\max}}\right) = 0. \tag{S5.13}$$

This occurs either when $b-a$ goes to minus infinity and hence $\gamma(a,b) = 0$, or when:

$$1 + \frac{2\gamma(a,b)^2}{p_{\max}^2} - 3\frac{\gamma(a,b)}{p_{\max}} = 0. \tag{S5.14}$$

Which can be solved straightforwardly using the quadratic formula:

$$\gamma(a,b) = \frac{\frac{3}{p_{\max}} \pm \sqrt{\frac{9}{p_{\max}^2} - \frac{8}{p_{\max}^2}}}{\frac{4}{p_{\max}^2}} \tag{S5.15}$$

or simplified:

$$\gamma(a,b) = \frac{(3\pm 1)p_{\max}}{4}. \tag{S5.16}$$

We use the definition of γ to solve for a relation between a and b:

$$p_{\max}\frac{1}{1+e^{-k(b-a-h)}} = \frac{(3\pm 1)p_{\max}}{4}, \tag{S5.17}$$

or:

$$1 + e^{-k(b-a-h)} = \frac{4}{3\pm 1}, \tag{S5.18}$$

Because $\frac{4}{3\pm1} = 1.5 \pm 0.5$, this is equivalent to

$$e^{-k(b-a-h)} = 0.5 \pm 0.5. \tag{S5.19}$$

This occurs when either $b-a$ goes to infinity, and so the left side goes to zero, or when the left side is equal to one, which corresponds to:

$$-k(b-a-h) = 0. \tag{S5.20}$$

Hence the line at which the curvature vanishes lies at:

$$b-a = h. \tag{S5.21}$$

In contrast, the values for $\overline{a}$ and $\overline{b}$ where the approximation predicts the largest difference to the naive estimate, occurs when the curvature reaches an extreme value. We start by calculating the maximal curvature in the a direction. We do so by setting the third order derivative to zero:

$$\frac{\partial^3\gamma(a,b)}{\partial a^3} = \frac{\partial}{\partial a}\frac{\partial^2\gamma(a,b)}{\partial a^2} = \frac{\partial}{\partial a}k^2(\gamma(a,b) + \frac{2\gamma(a,b)^3}{p_{\max}^2} - 3\frac{\gamma(a,b)^2}{p_{\max}}) = 0, \tag{S5.22}$$

which is equivalent to:

$$\frac{\partial\gamma(a,b)}{\partial a} + \frac{6\gamma(a,b)^2}{p_{\max}^2}\frac{\partial\gamma(a,b)}{\partial a} - 6\frac{\gamma(a,b)}{p_{\max}}\frac{\partial\gamma(a,b)}{\partial a} = 0. \tag{S5.23}$$

As a consequence, either

$$\frac{\partial\gamma(a,b)}{\partial a} = 0, \tag{S5.24}$$

which occurs when $\overline{a} \to \infty$ or $\overline{b} \to \infty$, or:

$$1 + \frac{6}{(1+e^{-k(b-a-h)})^2} - \frac{6}{1+e^{-k(b-a-h)}} = 0. \tag{S5.25}$$

We simplify this equation by defining $\eta = 1 + e^{-k(b-a-h)}$:

$$1 + \frac{6}{\eta^2} - \frac{6}{\eta} = 0. \tag{S5.26}$$

This can be written as a standard quadratic equation:

$$\eta^2 + 6 - 6\eta = 0. \tag{S5.27}$$

This is equivalent to:

$$(\eta - 3)^2 - 3 = 0, \tag{S5.28}$$

and hence:

$$\eta = 3 \pm \sqrt{3}. \tag{S5.29}$$

Putting the definition of η back in and solving for a gives:

$$a = b - h + \frac{\ln\left(2 \pm \sqrt{3}\right)}{k}. \tag{S5.30}$$

To show that the extrema are symmetric around the inflection line $a = b - h$ (see Eq. S5.21), we note that:

$$2 - \sqrt{3} = \frac{2 - \sqrt{3}}{4 - 3} = \frac{2 - \sqrt{3}}{(2 + \sqrt{3})(2 - \sqrt{3})} = \frac{1}{2 + \sqrt{3}} = (2 + \sqrt{3})^{-1}. \tag{S5.31}$$

Since $\ln(x^{-1}) = -\ln(x)$ we can therefore write:

$$a = b - h \pm \frac{\ln\left(2 + \sqrt{3}\right)}{k}. \tag{S5.32}$$

or:

$$b = a + h \pm \frac{\ln\left(2 + \sqrt{3}\right)}{k}. \tag{S5.33}$$

From Eq. 8, we can deduce the difference between the approximated value of γ and the naive value

as:

$$\overline{\gamma(a,b)} - \gamma(\overline{a},\overline{b}) = \left.\frac{\partial^2\gamma}{\partial a^2}\right|_{(\overline{a},\overline{b})} \left(\frac{1}{2}\sigma_a^2 + \frac{1}{2}\sigma_b^2 - \sigma_{a,b}\right) \tag{S5.34}$$

From this expression it is clear to see that when the trait variances and covariance are kept constant, the largest difference occurs when the curvature reaches an extreme value, which in turn occurs when:

$$\overline{a} = \overline{b} - h \pm \frac{\ln\left(2+\sqrt{3}\right)}{k}, \tag{S5.35}$$

as derived above. Whether the line corresponds to maximum or minimum curvature depends on the sign of the $\pm$.

S6 Lotka-Volterra competition model

S6.1 Equilibria and coexistence

We use a Lotka-Volterra competition model that is defined as follows:

$$\begin{aligned}\frac{\mathrm{d}N_A}{\mathrm{d}t} &= r_A N_A \left(1 - \frac{\alpha_{AA}N_A + \alpha_{AB}N_B}{K_A}\right)\\ \frac{\mathrm{d}N_B}{\mathrm{d}t} &= r_B N_B \left(1 - \frac{\alpha_{BB}N_B + \alpha_{AB}N_A}{K_B}\right),\end{aligned} \tag{S6.1}$$

with N_A and N_B the abundances of species A and B, r_i their intrinsic growth rates, and K_i their carrying capacities. Furthermore, α_{AA} and α_{BB} are the intraspecific interaction parameters whereas α_{AB} is the within species interaction parameter.

By setting both derivatives in Eq. S6.1 to zero, the 4 equilibria of the system can be found:

$$(N_A^*, N_B^*) = \begin{cases} (0,0) \\ (\frac{K_A}{\alpha_{AA}}, 0) \\ (0, \frac{K_B}{\alpha_{BB}}) \\ (\frac{\alpha_{BB}K_A - \alpha_{AB}K_B}{\alpha_{AA}\alpha_{BB} - \alpha_{AB}^2}, \frac{\alpha_{AA}K_B - \alpha_{AB}K_A}{\alpha_{AA}\alpha_{BB} - \alpha_{AB}^2}) \end{cases} \tag{S6.2}$$

Coexistence is possible when both species can invade a system in which only the other species is present, that is, if species B has a positive per-capita growth rate at the equilibrium with only species A $(\frac{K_A}{\alpha_{AA}}, 0)$, and species A has a positive per-capita growth rate in the equilibrium $(0, \frac{K_B}{\alpha_{BB}})$. Therefore, coexistence is possible when the conditions:

$$r_A \left(1 - \frac{\alpha_{AB}K_B}{\alpha_{BB}K_A}\right) > 0 \tag{S6.3}$$

$$r_B \left(1 - \frac{\alpha_{AB}K_A}{\alpha_{AA}K_B}\right) > 0, \tag{S6.4}$$

are both met. Since all parameters are positive, the condition for coexistence simplifies to $\frac{\alpha_{AB}}{\alpha_{BB}} < \frac{K_A}{K_B}$ and $\frac{\alpha_{AB}}{\alpha_{AA}} < \frac{K_B}{K_A}$. When one condition is met, but the other is not, only one of the species will be maintained. In particular, only species B is maintained when $\frac{\alpha_{AB}}{\alpha_{BB}} > \frac{K_A}{K_B}$ and $\frac{\alpha_{AB}}{\alpha_{AA}} < \frac{K_B}{K_A}$. Finally, when neither condition is met, only one of the species will persist depending upon intrinsic growth rates and starting densities. In the special case when carrying capacities are equal, $K_A = K_B$, coexistence will occur when $\alpha_{AB} < \min(\alpha_{AA}, \alpha_{BB})$ i.e. interspecific competition needs to be less than intraspecific competition for coexistence.

S6.2 ITV affecting only interspecific competition

We first focus on the case where only interspecific competition is affected by ITV by setting $\alpha_{AA} = \alpha_{BB} = 1$ and $\alpha_{AB} = E[\gamma_{AB}(a,b)] := \alpha$. The coexistence criterium now becomes $\alpha < \min(\frac{K_A}{K_B}, \frac{K_B}{K_A})$. The two species equilibrium lies at $(N_A^*, N_B^*) = (\frac{K_A - \alpha K_B}{1-\alpha^2}, \frac{K_B - \alpha K_A}{1-\alpha^2})$. Due to changes in the average interspecific competition coefficient, the equilibrium abundances change as well, as illustrated in

Fig. S6.1.

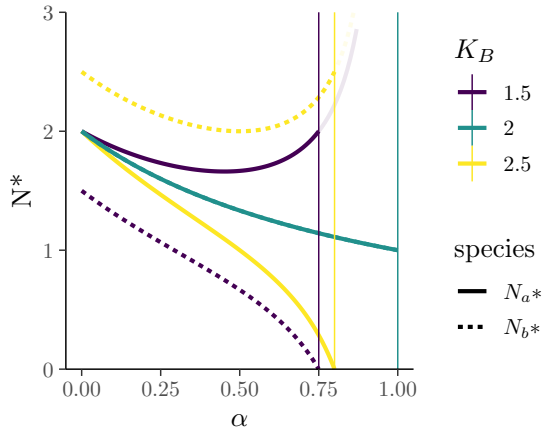

Figure S6.1 – Abundances at the coexistence equilibrium for the competition model at different competition strengths. $K_A = 2$, vertical lines correspond to the value of α at which the coexistence equilibrium becomes unstable. Note that when $K_A = K_B = 2$, the equilibrium abundances of the two species are equal and the two lines overlap.

For the special case when $K_A = K_B = K$, the coexistence becomes unstable when $\alpha \geq 1$, and the coexistence equilibrium thus only applies when $0 \leq \alpha < 1$. In this special case, the equilibrium densities can be simplified to $(N_A^*, N_B^*) = (\frac{K}{1+\alpha}, \frac{K}{1+\alpha})$. The equilibrium abundances of the two species are identical and decrease with α. Their value is between $K/2$ and K with the maximum equilibrium values occurring when interspecific competition is 0 ($\alpha = 0$). The minimum total equilibrium abundance of both species taken together is K.

We now turn to the more general case with unequal carrying capacities, in particular we set $K_A > K_B$ for the remainder of this section. When competition is negligible ($\alpha = 0$), the coexistence equilibrium is $(N_A^*, N_B^*) = (K_A, K_B)$. At the other extreme, at the point where coexistence becomes unstable ($\alpha = \frac{K_B}{K_A}$), species A, which has the higher carrying capacity, is at its carrying capacity, while species B goes extinct $(N_A^*, N_B^*) = (K_A, 0)$. The direction of change in equilibrium abundances

with increasing α can be found by evaluating the derivatives:

$$\frac{\mathrm{d}N_A^*}{\mathrm{d}\alpha} = K_B \left(2\alpha \frac{K_A}{K_B} - (1+\alpha^2)\right) / \left(1-\alpha^2\right)^2, \tag{S6.5}$$

$$\frac{\mathrm{d}N_B^*}{\mathrm{d}\alpha} = K_A \left(2\alpha \frac{K_B}{K_A} - (1+\alpha^2)\right) / \left(1-\alpha^2\right)^2. \tag{S6.6}$$

By setting the first derivative to 0, we find two potential extreme values for N_A at:

$$\hat{\alpha}_\pm = \frac{K_A}{K_B}\left(1 \pm \sqrt{1 - \frac{K_B^2}{K_A^2}}\right). \tag{S6.7}$$

Because we assumed that $K_A > K_B$, the argument in the square root can lie anywhere between 0 and 1, and therefore also the root is real and lies between 0 and 1. As a consequence the solution $\hat{\alpha}_+$ is larger than $\frac{K_A}{K_B}$, which itself is larger than $\frac{K_B}{K_A}$, and thus $\hat{\alpha}_+$ is larger than the maximum value at which the coexistence equilibrium can be stable. We now check under what conditions $\hat{\alpha}_-$ lies within the range $[0, \frac{K_B}{K_A}]$. It is obvious, with the square root being between 0 and 1 that $\hat{\alpha}_- > 0$. For the upper limit of the range, we evaluate:

$$\hat{\alpha}_- = \frac{K_A}{K_B}\left(1 - \sqrt{1 - \frac{K_B^2}{K_A^2}}\right) < \frac{K_B}{K_A}. \tag{S6.8}$$

We multiply both sides by the positive number $\frac{K_B}{K_A}$ and subtract 1, to find:

$$-\sqrt{1 - \frac{K_B^2}{K_A^2}} < \frac{K_B^2}{K_A^2} - 1. \tag{S6.9}$$

We now define a new variable $\eta = 1 - \frac{K_B^2}{K_A^2}$. Note that because $K_A > K_B$, η can only take values between 0 and 1. We also multiply the inequality with -1, thereby inverting the inequality sign:

$$\sqrt{\eta} > \eta \qquad \text{with } 0 < \eta < 1. \tag{S6.10}$$

This last inequality clearly holds for all values that η can take and therefore $\hat{\alpha}_-$ lies within the

range where the coexistence equilibrium is stable.

Given that (1) there is one extreme within the interval, (2) the derivative Eq. S6.5 is negative when $\alpha = 0$, and (3) the equilibrium value for N_A^* is equal to K_A both when $\alpha = 0$ and when $\alpha = \frac{K_B}{K_A}$, we conclude that this extreme value must be a minimum. Hence, N_A^* first decreases with increasing α until a turning point is reached after which it starts increasing towards its carrying capacity, K_A, again. Meanwhile, N_B^* strictly decreases with increasing α.

The equilibrium abundances at $\alpha = \hat{\alpha}$ are:

$$N_A^*|_{\alpha=\hat{\alpha}} = \frac{K_B^2}{2K_A\left(1 - \sqrt{1 - \frac{K_B^2}{K_A^2}}\right)} \tag{S6.11}$$

$$N_B^*|_{\alpha=\hat{\alpha}} = \frac{K_B}{2}. \tag{S6.12}$$

The larger the difference between K_A and K_B, the lower $\hat{\alpha}$ between the two species. And the lower the maximum competition, the higher the ratio $\frac{N_A^*}{K_A}$ while the ratio $\frac{N_B^*}{K_B}$ is always one half at $\hat{\alpha}$. The same arguments hold for species B if $K_B > K_A$, because due to the inherent symmetry of the system one can simply exchange the labels of the species.

S6.3 ITV affecting inter- and intraspecific competition

We now turn to the more general model, where both intra- and interspecific competition are affected by ITV. Now, each competition coefficient will be calculated using the estimation methods described in section S6.3.1 below, based on their specific interaction functions and trait distributions, and we set $\alpha_{AB} = E[\gamma_{AB}]$, $\alpha_{AA} = E[\gamma_{AA}]$, and $\alpha_{BB} = E[\gamma_{BB}]$. The average interspecific competition coefficient is calculated as in the main text. For the intraspecific competition coefficient of species A, we denote the joint distribution as $f_{AA}(a, a')$ which is defined as the meeting probability of an individual in species A, having phenotype a, with another individual of phenotype a' within the same species, with $\rho_{aa'}$ the correlation in trait values across meetings of individuals within the same species. For example, a positive correlation implies that individuals tend to meet with other individuals that have a similar trait value. Although our approach is not restricted to this, for the

results in this section we assume a bivariate normal distribution:

$$f_{AA}(a,a') = \frac{1}{2\pi\sigma_a^2\sqrt{1-\rho_{aa'}}} e^{-\frac{1}{2(1-\rho_{aa'})^2}\left[(\frac{a-\mu_a}{\sigma_a})^2 - 2\rho_{aa'}(\frac{a-\mu_a}{\sigma_a})(\frac{a'-\mu_a}{\sigma_a}) + (\frac{a'-\mu_a}{\sigma_a})^2\right]} \tag{S6.13}$$

The joint distribution of meeting probabilities for species B is defined analogously.

We describe each competition type with a Gaussian interaction function. For interspecific competition this interaction function is defined with parameters $c_{\max,AB}$ and ω_{AB} as follows:

$$\gamma_{AB}(a,b) = c_{\max,AB} e^{\frac{-(a-b)^2}{\omega_{AB}^2}} \tag{S6.14}$$

Intraspecific interactions in species A are described by the interaction function $\gamma_{AA}(a,a')$, which depends on the trait values a and a' of the two individuals of species A that meet and on the parameters $c_{\max,AA}$ and ω_{AA} as:

$$\gamma_{AA}(a,a') = c_{\max,AA} e^{\frac{-(a-a')^2}{\omega_{AA}^2}} \tag{S6.15}$$

Similarly, we can define an interaction function for species B denoted by $\gamma_{BB}(b,b')$ as:

$$\gamma_{BB}(b,b') = c_{\max,BB} e^{\frac{-(b-b')^2}{\omega_{BB}^2}} \tag{S6.16}$$

Note that when ω_{AA} and ω_{BB} tend to infinity α_{AA} and α_{BB} become equal to $c_{\max,AA}$ and $c_{\max,BB}$ respectively and are no longer trait dependent. When $c_{\max,AA} = c_{\max,BB} = 1$, the model reduces to the model in section 3.2.1 in the main text.

S6.3.1 Estimation of average interaction parameter $E[\gamma(a,b)]$

The naive and "true" estimates are obtained for each of the competition kernels separately, in the same way as in the model in the main text. Note, however, that due to the trait means for

intraspecific competition being equal (i.e. $\mu_a = \mu_a$), these naive estimates are not trait-dependent:

$$\gamma_{AA}(\overline{a}, \overline{a}) = c_{\max,AA} \tag{S6.17}$$

$$\gamma_{BB}(\overline{b}, \overline{b}) = c_{\max,BB}. \tag{S6.18}$$

Using Eq. 8, the second-order Taylor approximations are:

$$\overline{\gamma_{AB}(a,b)} \approx \gamma_{AB}(\overline{a}, \overline{b}) + \gamma_{AB}(\overline{a}, \overline{b}) \cdot \left(\frac{2(\overline{a} - \overline{b})^2 - \omega_{AB}^2}{\omega_{AB}^4} \right) \cdot \left(\sigma_a^2 + \sigma_b^2 - 2\sigma_{a,b} \right), \tag{S6.19}$$

$$\overline{\gamma_{AA}(a,a')} \approx c_{\max,AA} \left(1 - \frac{2\sigma_a^2}{\omega_{AA}^2} + \frac{2\sigma_{a,a'}}{\omega_{AA}^2} \right), \tag{S6.20}$$

$$\overline{\gamma_{BB}(b,b')} \approx c_{\max,BB} \left(1 - \frac{2\sigma_b^2}{\omega_{BB}^2} + \frac{2\sigma_{b,b'}}{\omega_{BB}^2} \right). \tag{S6.21}$$

Similar to the naive estimates, in these Taylor approximations, $\overline{\gamma_{AB}(a,b)}$ is dependent on the difference in trait means, whereas $\overline{\gamma_{AA}(a,a')}$ and $\overline{\gamma_{BB}(b,b')}$ do not depend on trait means.

ITV always decreases the intraspecific interaction parameters $\overline{\gamma_{AA}(a,a')}$ and $\overline{\gamma_{BB}(b,b')}$, whereas within species covariance (positive) always increases them. Note that for some combinations of variance, covariance, mean difference, and ω the second order Taylor approximation of inter- and intraspecific interaction parameters can become negative. Such regions are biologically infeasible and are not considered for coexistence or population dynamics.

S6.3.2 Results

As already observed in section S6.3.1, the mean interaction strength estimates (α's) are affected by ω's, $c_{\max}$'s, variances, co-variances, and $|\mu_a - \mu_b|$. Consequentially, whether the two competitors can coexist is also affected, as shown in Fig. S6.2. For simplicity, in this figure, we fixed the co-variances to zero and set $K_A = K_B$. The regions in Fig. S6.2 are calculated from the coexistence condition described in section S6.1. Note that the subplots in each panel of Fig. S6.2 are symmetric around $\sigma_a = \sigma_b$ barring the mirroring of A wins and B wins regions, where A wins when species A has

more variation than species B and vice versa. Moreover, in some subplots coexistence is favoured when both species have similar amounts of trait variation. As a consequence, when the amount of trait variation is much larger in one of the species, coexistence may be favoured by an increase in trait variation in the other species (e.g. second row from the top in the bottom right panel of Fig. S6.2) .

When variance is small, the coexistence predictions obtained from the second order Taylor approximation agree with those based on the sampling estimates. However, as the variances increase, the predictions from the approximation diverge from the "true" predictions from the sampling method. In particular when $\sigma_{ii} > \omega/\sqrt{2}$, the approximation predicts the associated intraspecific competition coefficient to be negative, as indicated by the red striped regions. For larger ω, the infeasible regions are smaller (Fig. S6.2).

When $\frac{\omega}{\sqrt{2}} > |\mu_a - \mu_b|$ (see Eq. S6.19), variance reduces the interspecific competition, and for large enough variance, α_{AB} becomes negative. This causes the infeasible regions in the respective approximation panels with fixed intraspecific competition in Fig. S6.2. On the other hand, α_{AB} increases with σ when $\frac{\omega}{\sqrt{2}} < |\mu_a - \mu_b|$ and hence does not become negative which leads to no infeasible regions in the respective approximation panel of fixed intraspecific competition.

Importantly, when we compare the results for fixed intraspecific competition (column 1, Fig. S6.2) with variable intraspecific competition (column 2, Fig. S6.2) we note that the coexistence regions shrink when both intra- and interspecific competition are affected by ITV. Similarly, within any subpanel, coexistence becomes less likely with increasing variances. This is expected behaviour, because in the used set up, interspecific competition is reduced less (and it is potentially even increased) than intraspecific competition. This finding is however dependent on intra- and interspecific competition acting in a similar manner. When competition width for intraspecific competition is much larger than for interspecific competition, the opposite effect can occur (see for an example Fig. S6.3).

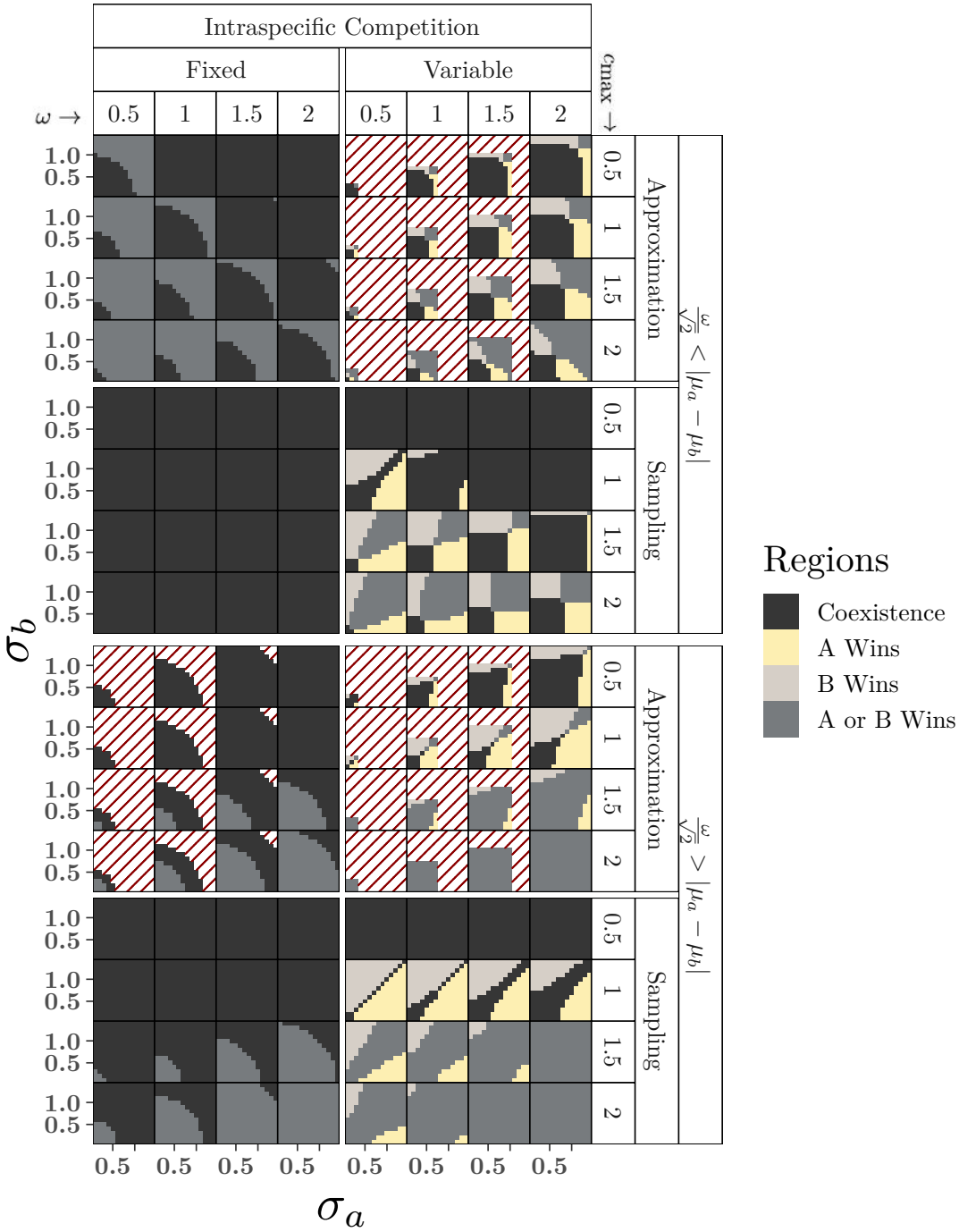

Figure S6.2 – The effect of variation in ITV (σ_a and σ_b), width (ω), and $c_{\max}$ on regions of coexistence. Red striped area is the infeasible region. The left column is for fixed intraspecific competition (i.e. $\alpha_{AA} = \alpha_{BB} = 1$), and the right column is for variable intraspecific competition. To ensure comparability between the two columns only the $c_{\max,AB}$ (here $c_{\max}$) is changed, and $c_{\max,AA}$ and $c_{\max,BB}$ are fixed to 1. $|\mu_a - \mu_b| = 1.5 \cdot \frac{\omega}{\sqrt{2}}$ under the condition $\frac{\omega}{\sqrt{2}} < |\mu_a - \mu_b|$ and $|\mu_a - \mu_b| = 0.5 \cdot \frac{\omega}{\sqrt{2}}$ under the condition $\frac{\omega}{\sqrt{2}} > |\mu_a - \mu_b|$. All the ω are equal (i.e. $\omega_{AB} = \omega_{AA} = \omega_{BB} = \omega$), carrying capacities $K_A = K_B = 500$, and correlation is kept zero.

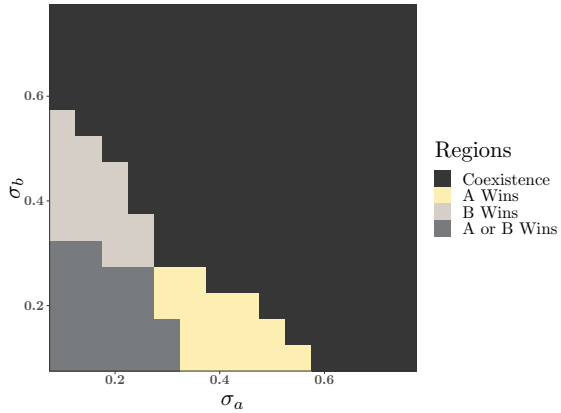

Figure S6.3 – An example of ITV-dependent inter- and intraspecific competition where higher variance promotes coexistence. Here, $\omega_{AB} = 0.4$, $\omega_{AA} = \omega_{BB} = 1$, $c_{\max,AB} = 1.5$, $c_{\max,AA} = c_{\max,BB} = 1$, $|\mu_a - \mu_b| = 0.05$, $\frac{K_A}{K_B} = 1$, and the sampling method is used for estimation of mean interaction.

S7 Predator-prey model

S7.1 Equilibria and coexistence

The system:

$$\begin{aligned} \frac{\mathrm{d}N_A}{\mathrm{d}t} &= r_A N_A (1 - \frac{N_A}{K}) - N_A N_B \phi \\ \frac{\mathrm{d}N_B}{\mathrm{d}t} &= r_B N_B + c N_A N_B \phi, \end{aligned} \tag{S7.1}$$

has three equilibrium points $(N_A^* = 0, N_B^* = 0), (N_A^* = K, N_B^* = 0)$ and $(N_A^* = \frac{-r_B}{c\phi}, N_B^* = \frac{r_A}{\phi}(1 + \frac{r_B}{c\phi K})$, where the third is the potential coexistence equilibrium where both species have non-zero abundance.

To determine whether coexistence is possible, we determine when prey have a positive per-capita growth rate when starting from zero abundance, with predators at their equilibrium value in the absence of prey (i.e. $N_B^* = 0$):

$$r_A > 0, \tag{S7.2}$$

and similarly when the predators have a positive per-capita growth rate when at zero abundance, with prey at their equilibrium value in the absense of predatore (i.e. $N_A^* = K$):

$$r_B + cK\phi > 0. \tag{S7.3}$$

Since r_A is always positive (convention), the condition for coexistence becomes:

$$\phi > -\frac{r_B}{cK}. \tag{S7.4}$$

Changes in ϕ due to ITV may thus affect the coexistence status of the two species in either direction, depending on the threshold location and the direction and magnitude of the effect of ITV on ϕ. For example a decrease in ϕ below the threshold in value in (12) leads to predator extinction making the second equilibrium ($N_A^* = K, N_B^* = 0$) asymptotically stable as the remaining equilibria becomes unstable.

The equilibrium abundances change with ϕ as evidenced by their derivatives:

$$\frac{\mathrm{d}N_A^*}{\mathrm{d}\phi} = \frac{r_B}{c\phi^2} < 0 \quad \text{for } r_B < 0 \tag{S7.5}$$

$$\frac{\mathrm{d}N_B^*}{\mathrm{d}\phi} = -\frac{r_A}{\phi^2}(1 + \frac{2r_B}{c\phi K}). \tag{S7.6}$$

By setting Eq. S7.6 equal to zero, it can be shown that the equilibrium abundance has an extremum at $\hat{\phi} = -\frac{2r_B}{cK}$. Here, $N_B^* = -\frac{r_A cK}{4r_B}$. The value of the second derivative negative at $\hat{\phi}$ ($-r_A\hat{\phi}^{-3}$) is negative and thus the equilibrium abundance is a maximum. The corresponding value of $N_A^* = \frac{K}{2}$, is half the carrying capacity for the prey species.

S7.2 Density-dependent interaction functions

We will now consider the example of a predator-prey model with a type-2 functional response such as the Rosenzweig-MacArthur model

$$\frac{\mathrm{d}N_A}{\mathrm{d}t} = r_A N_A \left(1 - \frac{N_A}{K}\right) - \frac{\epsilon N_A}{1 + \epsilon t_h N_A} N_B \tag{S7.7}$$

$$\frac{\mathrm{d}N_B}{\mathrm{d}t} = r_B N_B + c \frac{\epsilon N_A}{1 + \epsilon t_h N_A} N_B. \tag{S7.8}$$

Here A is the prey species with density N_A, intrinsic growth rate r_A and carrying capacity K and B is the predator species with density N_B, intrinsic growth rate r_B, which is usually assumed to be negative. The predation terms depend on the encounter rate ϵ, the handling time t_h and the conversion factor from prey individuals to predator individuals c.

The form of the functional response, i.e. the number of prey individuals consumed per predator per time unit, is derived by considering the time budget of an individual predator. If we assume that the predator searches prey for a time T_s, it will encounter $T_s \epsilon N_A$ prey. It will then need time $T_s \epsilon N_A t_h$ to handle these prey items. Thus the number of prey consumed per time unit taking into account both searching and handling is

$$F(N_A) = \frac{T_s \epsilon N_A}{T_s + T_s \epsilon N_A t_h} = \frac{\epsilon N_A}{1 + \epsilon t_h N_A}. \tag{S7.9}$$

S7.2.1 Incorporating intraspecific variation

Now, let us take into account intraspecific variation in both predator and prey. Assume that the traits in the two species vary independently, such that we can write the joint trait distribution as the product of the marginal distributions:

$$f_{AB}(a, b) = f_A(a) f_B(b). \tag{S7.10}$$

We assume that these traits influence the encounter rate, such that the encounter rate of a predator with trait b and a prey with trait a is $\epsilon(a, b)$.

Let $F(N_A, b)$ be the number of prey consumed per time unit for a predator with trait value b. Taking into account all possible prey traits and using the same arguments as for the case without variation,

$$F(N_A, b) = \frac{\int \epsilon(a,b) f_A(a) \mathrm{d}a N_A}{1 + t_h \int \epsilon(a,b) f_A(a) \mathrm{d}a N_A}. \tag{S7.11}$$

The total average rate at which predators consume prey is then

$$F(N_A) = \int F(N_A, b) f_B(b) \mathrm{d}b. \tag{S7.12}$$

The integral can again be computed numerically, but it depends on the current prey density N_A and thus would have to be recalculated as the prey density changes through time. To allow for an efficient numerical solution of ODEs using Eq. S7.12, we computed $F(N_A)$ over a range of values of N_A (100 values between 0 and K, the prey carrying capacity) and then used linear interpolation between them. We checked that using a finer grid did not noticeably alter the results.

S7.2.2 Approximation

To derive an approximation for $F(N_A)$, we again use second-order Taylor expansions. We first use

$$\epsilon(a,b) \approx \epsilon(\overline{a}, b) + \epsilon_a(\overline{a}, b)(a - \overline{a}) + \frac{1}{2}\epsilon_{aa}(\overline{a}, b)(a - \overline{a})^2 \tag{S7.13}$$

to approximate

$$\int \epsilon(a,b) f_A(a) \mathrm{d}a \approx \epsilon(\overline{a}, b) + \frac{1}{2}\epsilon_{aa}(\overline{a}, b)\sigma_a^2 := \nu(b), \tag{S7.14}$$

and thus

$$F(N_A, b) \approx \frac{\nu(b)}{1/N_A + t_h \nu(b)}. \tag{S7.15}$$

Finally, using a Taylor expansion in b around $\overline{b}$, we obtain

$$F(N_A) = \int F(N_A, b) f_B(b) \mathrm{d}b \approx F(N_A, \overline{b}) + \frac{1}{2} F_{bb}(N_A, \overline{b})\sigma_b^2. \tag{S7.16}$$

Then

$$F_b(N_A, b) \approx \frac{\partial}{\partial b} N_A(\nu(b)^{-1} + t_h N_A)^{-1}. \tag{S7.17}$$

Using the chain rule this becomes:

$$F_b(N_A, b) \approx -N_A \left((\nu(b)^{-1} + t_h N_A)^{-2}\right)\left(-\nu(b)^{-2}\right)\frac{\partial \nu(b)}{\partial b} = \frac{N_A}{(1 + t_h N_A \nu(b))^2}\frac{\partial \nu(b)}{\partial b}. \tag{S7.18}$$

Now using the product rule, we find for the second order derivative:

$$F_{bb}(N_A, b) \approx N_A(1 + t_h N_A \nu(b))^{-2}\frac{\partial^2 \nu(b)}{\partial b^2} - 2t_h N_A^2(1 + t_h N_A \nu(b))^{-3}\left(\frac{\partial \nu(b)}{\partial b}\right)^2 \tag{S7.19}$$

$$= \frac{\frac{\partial^2 \nu(b)}{\partial b^2}(\frac{1}{N_A} + t_h \nu(b)) - 2t_h\left(\frac{\partial \nu(b)}{\partial b}\right)^2}{N_A\left(\frac{1}{N_A} + t_h \nu(b)\right)^3}, \tag{S7.20}$$

where $\frac{\partial \nu(b)}{\partial b} = \epsilon_b(\overline{a}, b) + \frac{1}{2}\sigma_a^2 \epsilon_{aab}(\overline{a}, b)$ and $\frac{\partial^2 \nu(b)}{\partial b^2} = \epsilon_{bb}(\overline{a}, b) + \frac{1}{2}\sigma_a^2 \epsilon_{aabb}(\overline{a}, b)$. Note that unlike for the Taylor approximations presented in the main text, the first derivatives do not vanish in this approximation, suggesting that ITV can have an effect even if $\epsilon(a, b)$ is linear (though of course the form of the functional response is introducing nonlinearity).

Unlike the integrals and approximations in the main text, it appears that these formulas would need to be rederived for each model and may depend on the underlying assumptions about individual-level processes.

S7.2.3 Stability analysis

Given the the functional response function $F(N_A)$, derived either from the naive, the true, or the approximation method, we can write the dynamical system as

$$\frac{\mathrm{d}N_A}{\mathrm{d}t} = r_A N_A\left(1 - \frac{N_A}{K}\right) - F(N_A)N_B \tag{S7.21}$$

$$\frac{\mathrm{d}N_B}{\mathrm{d}t} = r_B N_B + cF(N_A)N_B. \tag{S7.22}$$

The system has two equilibria. At the first equilibrium, the prey is at its carrying capacity

($N_A^* = K$) and the predator is absent ($N_B^* = 0$). At the second equilibrium, the coexistence equilibrium,

$$F(N_A^*) = -\frac{r_B}{c} \tag{S7.23}$$

and

$$r_A N_A^* \left(1 - \frac{N_A^*}{K}\right) + \frac{r_B}{c} N_B^* = 0 \tag{S7.24}$$

$$\Leftrightarrow N_B^* = -\frac{c}{r_B} r_A N_A^* \left(1 - \frac{N_A^*}{K}\right). \tag{S7.25}$$

For each of the three methods, we computed N_A^* by numerically solving (S7.23) with the respective functional response and then N_B^* follows. Note that for the naive and the approximation also an exact expression for N_A^* can be obtained.

The stability of the prey-only equilibrium is assessed by checking whether or not the predator has a positive per-capita growth rate when the prey is at its carrying capacity. That is, the prey-only equilibrium is stable if

$$r_A + cF(K) < 0. \tag{S7.26}$$

To determine the stability of the coexistence equilibrium, we compute the Jacobian

$$\mathbf{J} = \begin{pmatrix} r_A - \frac{2r_A N_A}{K} - N_B \frac{\mathrm{d}F}{\mathrm{d}N_A} & -F(N_A) \\ cN_B \frac{\mathrm{d}F}{\mathrm{d}N_A} & r_B + cF(N_A) \end{pmatrix}. \tag{S7.27}$$

At the coexistence equilibrium,

$$\mathbf{J} = \begin{pmatrix} r_A - \frac{2r_A N_A^*}{K} - N_B^* \left.\frac{\mathrm{d}F}{\mathrm{d}N_A}\right|_{N_A^*} & \frac{r_B}{c} \\ cN_B^* \left.\frac{\mathrm{d}F}{\mathrm{d}N_A}\right|_{N_A^*} & 0 \end{pmatrix}. \tag{S7.28}$$

The coexistence equilibrium is stable if all eigenvalues have negative real parts.

The system's behaviour is then classified based on the stability of the prey-only equilibrium and the coexistence equilibrium. If the prey-only equilibrium is unstable, we classify the outcome as predator extinction. If the prey-only equilibrium is unstable and the coexistence equilibrium

is stable, we have stable coexistence at constant frequencies. And if both equilibria are unstable, we have coexistence with oscillations. For all cases shown in the figures, we also confirmed the classification through visual inspection of the time series.

S7.2.4 Results

We now illustrate the effect of ITV and the quality of the approximation using the logistic interaction function. Figure S7.1 shows the effect of ITV and the quality of the Taylor approximation on $F(K)$, the prey consumption per predator individual when the prey is at its carrying capacity. This is the quantity that determines whether or not the predator can persist. The figure uses the same values for trait means and standard deviations as Fig. 3e_2 and e_3 in the main text. There, without density dependence, the effect of ITV is similar for predator-prey size differences above or below h, the difference in trait values where the curvature of the interaction function disappears. Furthermore, an increase in prey standard deviation has the same effects as an increase in predator standard deviation. With density dependence, in contrast, the effect of ITV is stronger when the average predator-prey size difference is below h and increasing the standard deviation in prey traits has much larger effects than increasing the standard deviation of predator traits. As an intuitive explanation, when the average predator-prey size difference is larger than h, a large part of the prey population is within the predators' reach and as a consequence, the predators function close to the maximum number of prey that they can handle per time unit. When trait variation in prey increases, the small number of prey that is now no longer in the reach of the predators has a very minor effect on the total average predation. In contrast, when the average predator-prey size difference is below h, predation is mainly governed by searching time. In contrast to the handling time, searching time directly depends on the number of prey available. If through trait variation the number of prey items within reach changes, this is expected to have a much stronger effect on the total predation in the system. Because the logistic interaction function used here has positive curvature when the interaction coefficient is low and negative curvature when the interaction function is high, the positive effects of ITV on the interaction coefficient are generally higher than the negative effects. This may be different for other interaction functions. The Taylor approximation generally is in good

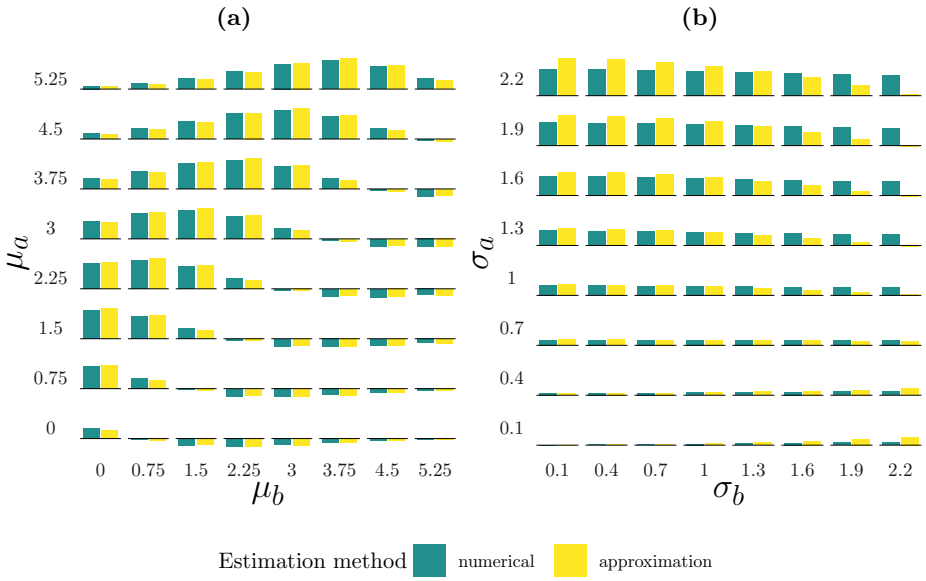

Figure S7.1 – Effect of prey and predator mean trait values and trait variation on $F(K)$, the predator's per-capita prey consumption at prey carrying capacity under the logistic interaction function. This quantity determines whether the prey-only equilibrium is stable or whether the predator can invade. Parameter values: $p_{max} = 0.1, k = 1, h = 1.5, r_A = 1, r_B = -0.3, c = 0.03, K = 1000, t_h = 0.05$. In (a) $\sigma_a = \sigma_b = 1$. In (b) $\mu_a = 2.5$ and $\mu_b = 2$. The scale of the effects differs between (a) and (b). In (a), the maximum absolute difference between naive and true approach is about 1.7 and in (b) 3.4.

agreement with the "true" numerical approach, except in cases with high standard deviations, as expected.

For the scenarios in Fig. S7.1a, the stability analysis showed that the outcome is predator extinction if the predator is small relative to the prey, coexistence with oscillations if the predator is much larger than the prey, and a stable coexistence equilibrium (no oscillations) if the predator is only slightly larger than the prey (Fig. S7.2). Qualitatively, this was the case for all three approaches (naive, numerical, and approximation), but the naive approach predicted predator extinction in some cases where both numerical approach and approximation predicted a stable coexistence outcome. For the scenarios in Fig. S7.1b, predator extinction was predicted in most cases by all three approaches, but the numerical approach and approximation predicted coexistence at a stable equilibrium in a few cases, with slight differences among the two (Fig. S7.2). All classifications were

checked through visual inspection of the time series. A few example time series and the corresponding functional response curves are shown in Fig. S7.3.

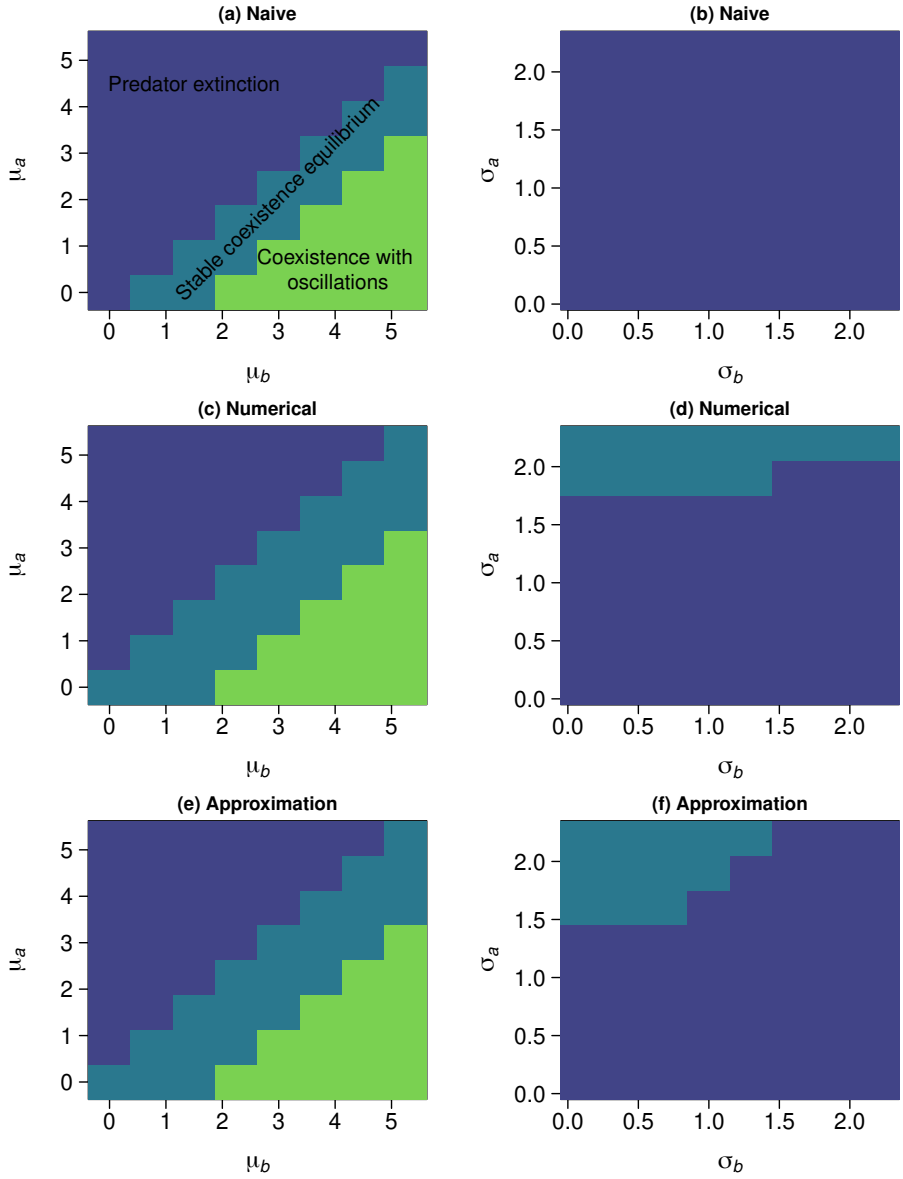

Figure S7.2 – Qualitative outcomes in the dynamical systems corresponding to Fig. S7.1. Parameter values as in Fig. S7.1.

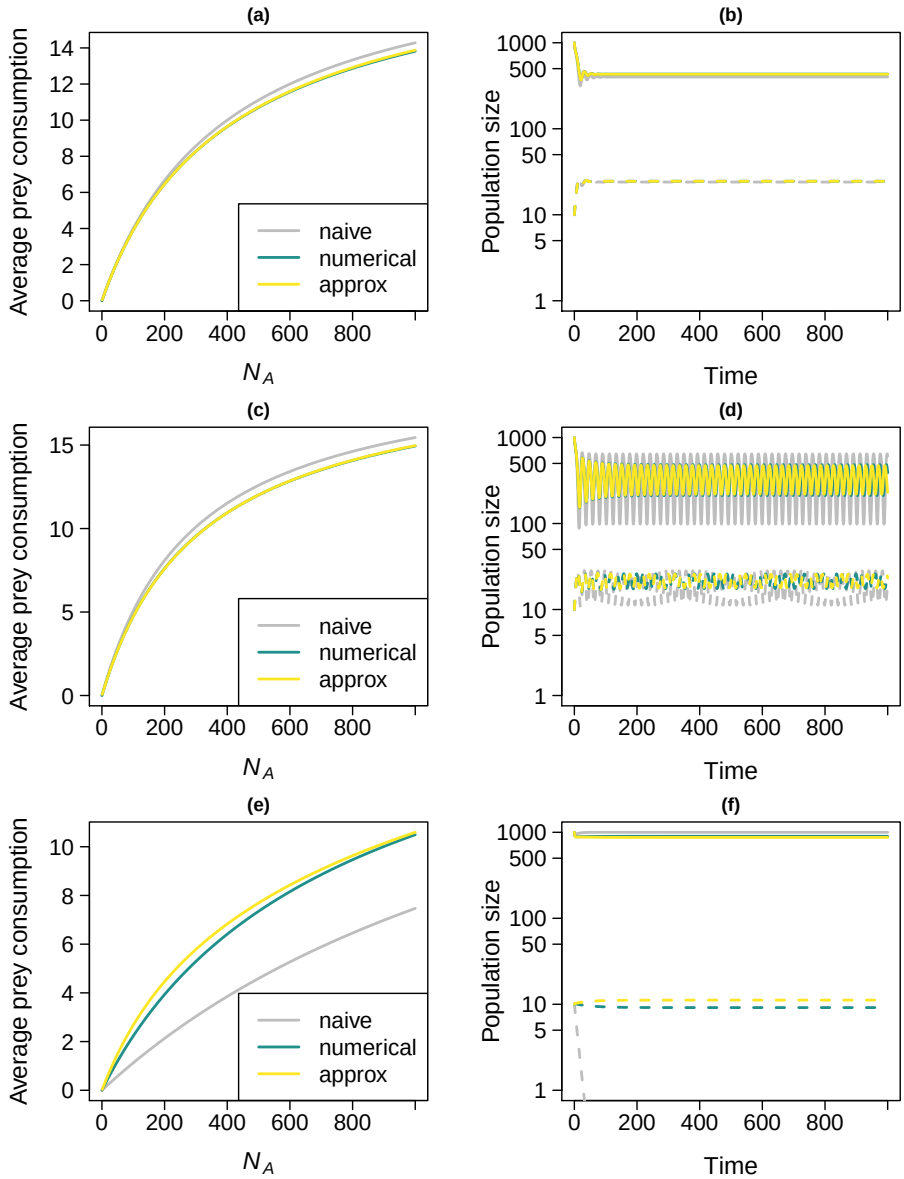

Figure S7.3 – Functional response curves (left column) and time series (right column) for three example scenarios. First row: $\mu_a = 2.25, \mu_b = 3.75, \sigma_a = 1, \sigma_b = 1$. Second row: $\mu_a = 0.75, \mu_b = 3.00, \sigma_a = 1, \sigma_b = 1$. Third row: $\mu_a = 2.2, \mu_b = 1.3, \sigma_a = 2.5, \sigma_b = 2$. Other parameters as in Fig. S7.1. Note that also the predator populations in (d) cycle between two densities. The long-term patterns are an artifact of the dashed line type.